Modelization and simulation of the mechanic behaviour of a cold water pipe submitted to heave and current along the water column, for applications to OTEC and offshore industry

Auteur : Panvalkar, Mihir
Promoteur(s) : 15002
Faculté : Faculté des Sciences appliquées
Diplôme : Master : ingénieur civil mécanicien, à finalité spécialisée en "Advanced Ship Design"
Année académique : 2020-2021
URI/URL : http://hdl.handle.net/2268.2/13646

Modelization and Simulation of the Mechanic Behaviour of a Cold Water Pipe submitted to Heave and Current along the water column, for applications to OTEC and Offshore Industry

Master's Thesis

EXECUTIVE REPORT

Submitted on: September 5, 2021
By: PANVALKAR Mihir || 24,Dhanvantari Nagar,Indore(M.P)-452012,India
e-mail: mihirpanvalkar@gmail.com
Student ID: S193301

Supervisor: Matthieu HOARAU, Engineer at the head of DEEPRUN
           Lucas VATINEL, Engineer at DEEPRUN
           Prof. Miloud BESSAFI, Director of Energy Lab
           Valentin ARRAMOUNET, Engineer at Innosea

Reviewer: Assoc Prof. PhD Sandita PACURARU, Dunarea de Jos University of Galati
           Domneasca Street, no.47, Galati ROMANIA(800008)

           Prof. Maciej TACZALA, West Pomeranian University of Technology
           Faculty of Maritime Technology and Transport, Szczecin, POLAND

Acknowledgements

Abstract

The study aims to determine the preliminary hydrodynamic analysis of the cold water pipe using an in-house built software cPendulum. The code cPendulum includes the influence of the design load coming from hydrodynamic forces coupled to an Ocean Thermal Energy Conversion (OTEC) floating Plant.

Firstly, the work defines the design considerations for the cold water pipe and the influence it has on the hydrodynamic coefficients .Then the design loads such as Morison's force along with Platform Motion are determined and implemented in the code cPendulum.

Furthermore, the work details about the selection of a mooring system designed to withstand the cyclonic conditions and the impact it will have on the platform behaviour. Moreover, as the oceanic waves are chaotic, the implementation of irregular waves in cPendulum is done to simulate a real scenario.

Finally, all parameters are implemented in cPendulum to analyse the behaviour of cold water pipe to draw the first conclusions about the efforts induced by the marine environment on the CWP[1].

---

[1]Cold Water Pipe

Contents

List of Figures

List of Tables

Glossary

CWP   Cold Water Pipe

ETM   Energie Thermique des Mers/Thermal Energy of the Seas

Low-tech Using machines, equipment, and methods that are not the most advanced

OTEC   Ocean Thermal Energy Conversion

FFT   Fast Fourier Transform

CFD   Computational Fluid Dynamics

ULS   Ultimate Limit States

ALS   Accidental Limit States

RAO   Response Amplitude Operator

HDPE   High Density Polyethylene

SHOM   Hydrographic and Oceanographic Service of the Navy

IFREMER   French research institute for the exploitation of the sea

Declaration of Authorship

I declare that this thesis and the work presented in it are my own and have been generated by me as the result of my own original research.

Where I have consulted the published work of others, this is always clearly attributed.

Where I have quoted from the work of others, the source is always given. With the exception of such quotations, this thesis is entirely my own work.

I have acknowledged all main sources of help.

Where the thesis is based on work done by myself jointly with others, I have made clear exactly what was done by others and what I have contributed myself.

This thesis contains no material that has been submitted previously, in whole or in part, for the award of any other academic degree or diploma.

I cede copyright of the thesis in favour of the Polytechnic University of Madrid and University of Liege.

September 5, 2021

Chapter 1

Introduction

Producing electricity in a long-term manner has become a necessity in recent decades to meet the needs of the population. Reunion Island, a French overseas territory in the Indian Ocean near Mauritius and Madagascar, has seen an increase in energy demand per person and population in recent years. Reunion Island relies on coal and fuel imports to meet its energy needs. To meet this requirement, investments are made to develop the use of renewable energy to rise the energy autonomy [1]. Today, about 36 % of the electricity produced in Reunion Island comes from renewable energy. However, the massive use of intermittent energies such as photovoltaics causes instabilities in the grid. Therefore, the use of intermittent renewable energy is limited [1] and new projects have to integrate a storage unit. As a result, Ocean Thermal Energy Conversion (OTEC), a non-intermittent renewable energy resource, appears to be an attractive alternative for territories with no interconnected grid, such as Reunion Island.

1.1 Ocean Thermal Energy Conversion

On the one hand, seawater on the surface stores solar energy and has a constant temperature through the day and at night (in Reunion Island 28°C in summer and 23°C in winter). On the other hand, the deep sea water is cold (around 5°C at a depth of 1000m) and easily accessible near the coast. OTEC uses this temperature difference as an energy source to generate electricity.

As shown in Figure 1.1, ocean thermal energy conversion is a process that uses the natural temperature gap in the depth of the ocean to generate clean and reliable electricity constantly all day long. The supply of warm water from the surface heated by the sun and of cold one from the bottom of the ocean activates a thermodynamic Rankine cycle producing electricity. To have a good enough efficiency for commercial use, this cycle requires a temperature difference of at least 20°C which makes it interesting in tropical areas where it can work all year round [2].

However, despite the optimal conditions in tropical areas such as Reunion Island where the temperature gradient of the water is the highest on Earth, it is still necessary to pump water from a depth of around 1000 meters. This is the main obstacle to the development of OTEC[1], as it requires the construction of a one kilometer vertical pipe, which is technologically feasible but very expensive.

OTEC plants are of two categories depending upon the selected site and requirement of environment conditions. There are onshore power plant and offshore power plant as represented in the Figure 1.2. For an onshore plant, the pipe is laid on the ground and is therefore longer (its length depends on the configuration of the sea bed). In the case of an offshore power plant,

---

[1]Ocean Thermal Energy Conversion

HOW OTEC WORKS
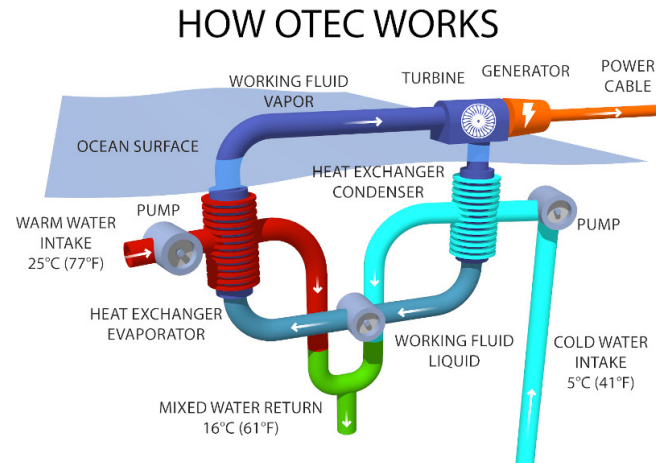
Figure 1.1: OTEC working principle

this pipe plunges vertically to the depth of the ocean but is subject to multiple forces (weight, platform movements, wave pressure, etc.). DEEPRUN aims to provide a technological solution to the main limitations of offshore based OTEC, which is the production of a kilometer-long cold water pipe.
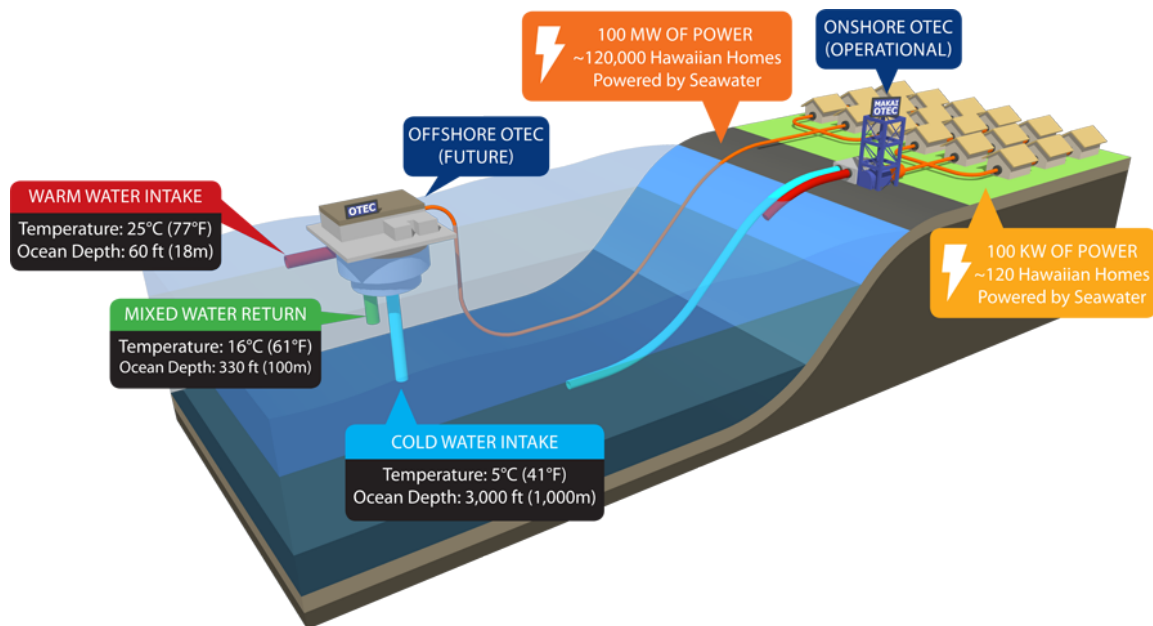
Figure 1.2: OTEC power plants

1.2   RUNETM project

The RUNETM project is based on development of a low-cost cold water pipe based on the Low-tech[2] principle. This disruptive approach envisages being able to produce the pipe locally

---

[2]Using machines, equipment, and methods that are not the most advanced

with materials available in the areas where the power plants are located. This approach differs from the existing companies who currently produce pipes designed for the para-petroleum industry, using high-tech materials, with lifetimes of several tens or even hundreds of years but prohibitive costs unsuited to the OTEC field.

The estimated lifespan of the CWP would vary from 2 to 5 years but it could easily be built and repaired on site in just a few days.The global design of the pipe is already established, with main focus on acquiring the material available in Reunion Island. The challenge is now to adapt this design and the materials used to make it possible to offer a Low-tech pipe that can be easily produced on site and that has an adequate lifespan.

1.3   Objectives of this study

The main objective of this study is to determine the global behaviour of the cold water pipe which is subjected to design loads coming from hydrodynamics force and platform motion using analytical and numerical tools.

The youthfulness of the project and its originality made it necessary to first lay the groundwork to clearly define the environmental conditions in which the OTEC plant will be installed. This being done, the technical study on itself could start on a sound basis.

Firstly, design considerations are defined to give the holistic view about the pipe. Then various design loads are defined which are going to determine the behaviour of the pipe. Furthermore, the study of Platform Amplitude of motion needs to be carried out to determine the loads coming from platform movements.

The agglomeration of these design loads will be used to analyse the coupled motion of the platform and CWP under regular and irregular waves to understand the real scenario subjected oceanic conditions. At the end of the study, the outputs of the hydrodynamic study are used as input in the structural study.

Chapter 2

Design Consideration

2.1 Global Dimensions

The proposed cold water pipe design is maintained to have Low-tech concept using local materials which must be able to be installed on site with limited machinery and an easily trained workforce [1]. The pipe is designed to pump water for an OTEC Power Plant of 2 MW. For this purpose, it needs to pump 25000 m^3/h of both warm and cold water, with a difference of temperature between them of 20 °C.

In the selected site offshore Reunion Island, the water temperature is higher than 25 °C at the surface and lower than 5 °C at 1000 m depth.

Thus, the length of the pipe is 1000 meters. It is divided in 1000 similar modules of 1 m height. As the flow rate of pumped water is chosen equal to 1m/s to limit the pressure drop, the diameter of the pipe is 2.5 m. The pipe is connected to a surface platform at its upper end and left hanging at its lower end making it clamped at one end.

The OTEC power plant and its appendages from a global point of view are shown in the following Figure 2.1:
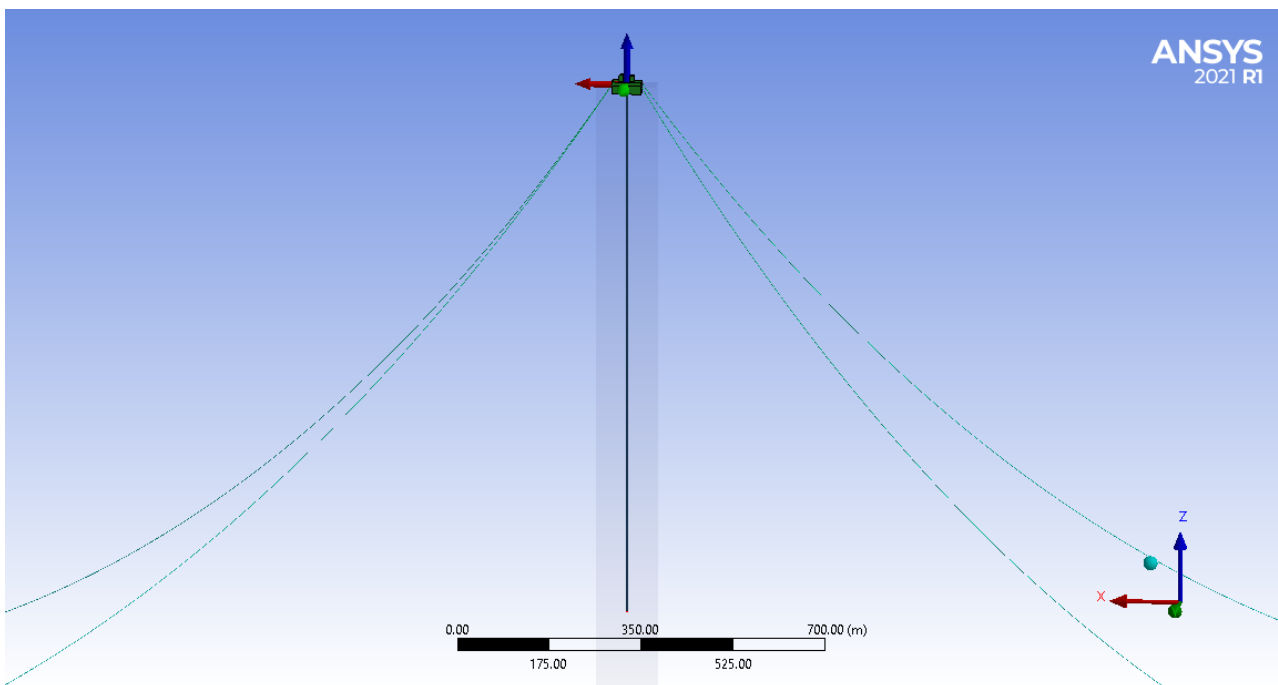
Figure 2.1: OTEC Power Plant with its mooring lines and CWP

---

[1]**Due to the confidentiality conditions, the CWP design is not being published in this version of report.**

2.2   Study approach

The study of the system is separated in two linked parts which are: on the one hand the hydrodynamics and on the other hand the structural study. These two have a reciprocal influence and hence, decided to proceed by loop. Indeed, each result leads to a potential evolution of the design and thus has an influence on the whole calculation. This is why it was decided, at the beginning of each loop, to fix the design, to carry out all calculations on this basis, and then at the end to compile all results to make the CWP evolve as explained in Figure 2.2. These steps are repeated until an optimal configuration is obtained.
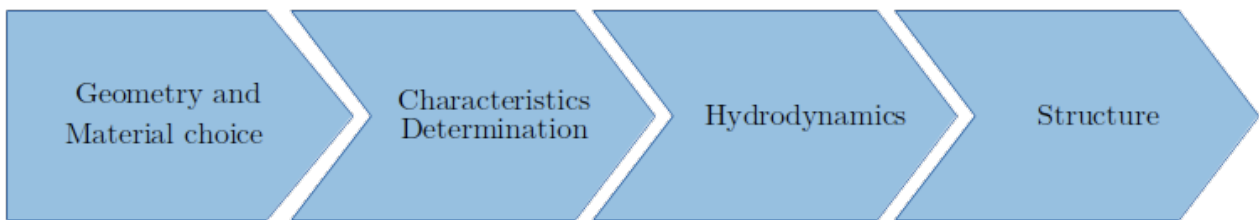
Figure 2.2: Methodology of a loop

The following study deals with the first iteration which were the longest to set up because it is at these stages that many decisions had to be taken and then improved in the following iterations. The steps followed to carry out the hydrodynamics analysis of the cold water pipe involved:

- Selection of Environmental Conditions

- Schematization of the ambient hydrodynamics

- Schematization of CWP's Structure

- Computation of Resulting Forces

- Determination of the dynamic of CWP

- Analysis of the results

These steps will be applied into practice for carrying out the thesis work.

2.3   Environmental Data

2.3.1   Site Selection

The place of OTEC plant installation needs to have specific requirements to be met because it affects the performance of the OTEC plant and defines the environmental conditions to which

the plant and the pipeline will be subjected.

The plant location that is selected for the installation of OTEC platform is along the coast of the city Le Port in Reunion Island, which is shown in Figure 2.3.
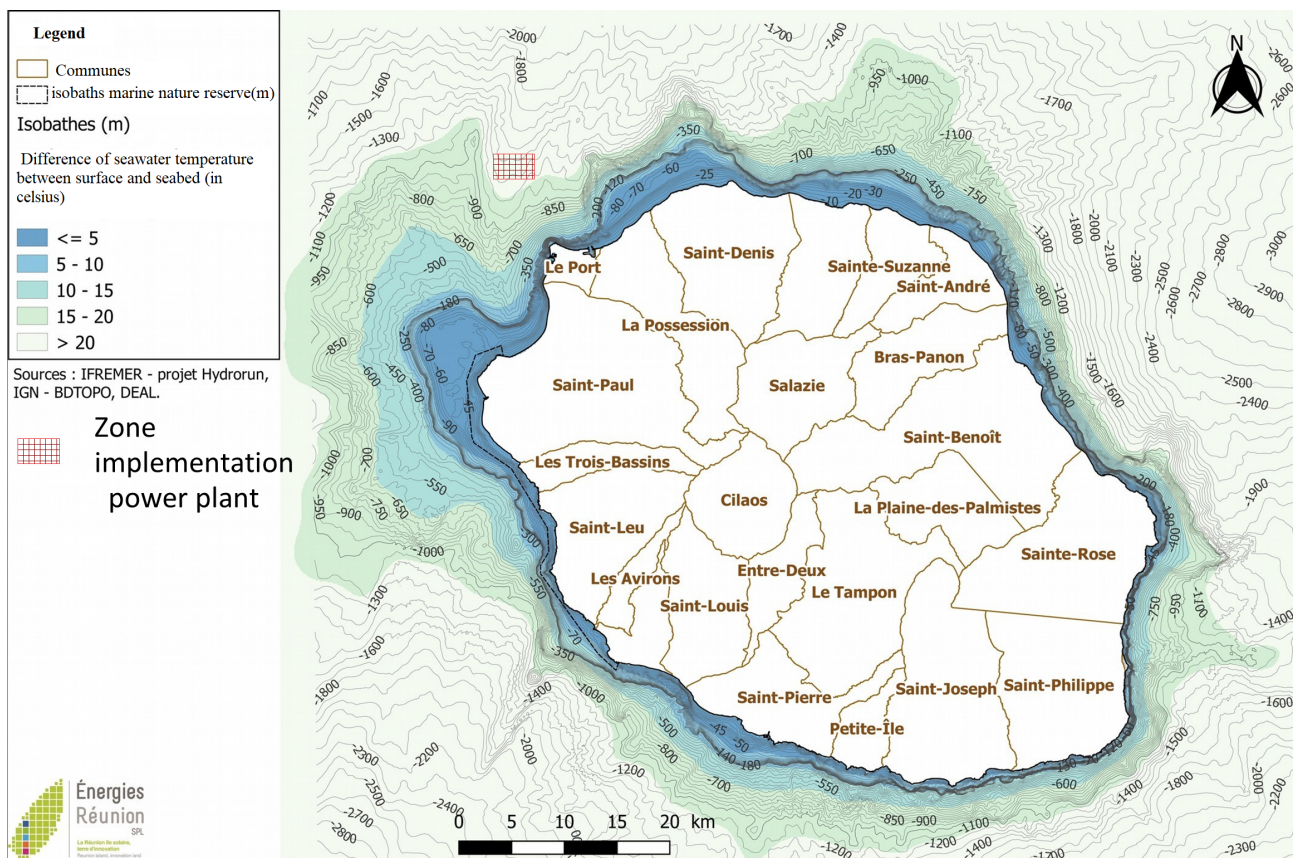
Figure 2.3: Geolocation of the proposed plant location area against a map background representing the temperature difference between the seabed and the sea surface

The reasons why the marked site in Figure 2.3 was selected are as follows:

- Close to the land and especially to the port and it's infrastructure

- Depth from 1300 to 1400m

- Temperature difference between bottom and surface area greater than 20 degrees

- Less vulnerable to yearly storms

- Swell type

2.3.2 Swell

Reunion Island is subject to three types of swells, as shown in Figure 2.4. The trade wind swell comes from south-easterly winds. It is common throughout the year on the south and east coasts and is characterized by small to medium amplitudes and short periods. The area near the port is protected from this swell.
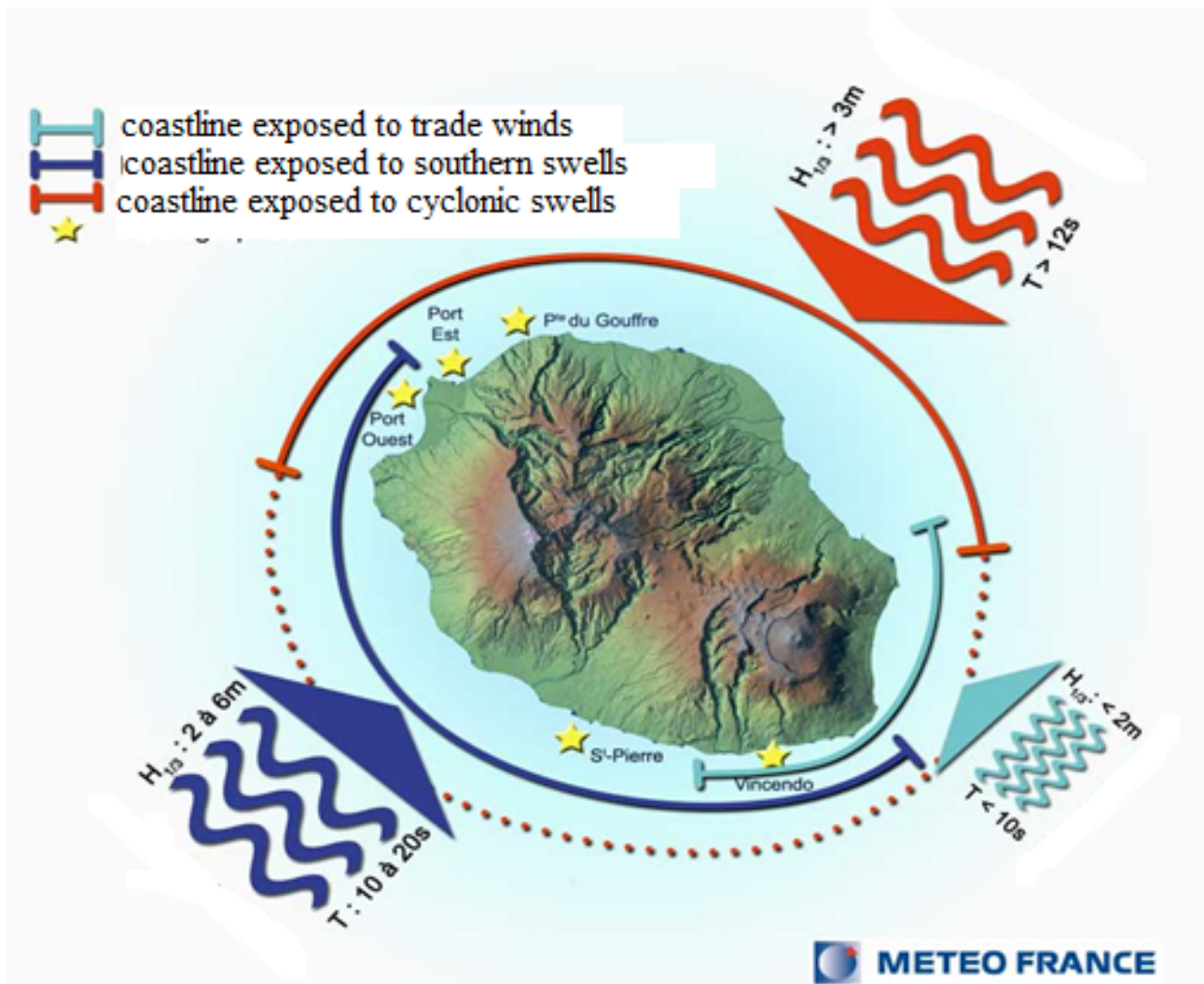
Figure 2.4: Types of swells in Reunion Island

The southern swell, with a high amplitude of up to 6 m and a period of up to 20 seconds, is the result of disturbances taking place in the south of South Africa. Important episodes occur 5-10 times a year. Its main direction is 40 degrees south, so it will not reach the area in the majority of cases. However, the direction can rise to 55 degrees south and reach the area.

The cyclonic swell generated by storms and tropical cyclones is of high amplitude and period. It reaches the north and east coasts of the island, and this is less than 5 times a year.

2.3.3   Consideration of Tropical Cyclones

The phenomenon of the cyclone is predictable several days in advance. Thus, in the case of a strong swell forecast, the idea is to detach the pipe from the platform when a cyclone is announced and to submerge it at a sufficient depth as DEEPRUN's CWP is not designed to resist to violent tropical cyclones. Thus, the environmental conditions surveyed are split in two categories:

- The operational conditions, corresponding to conditions not met 99.5% of the time. When the forecast predicts the worst conditions, the pipe is submerged.

- The cyclonic conditions, corresponding to the most extreme conditions surveyed at the zone of implantation of the power plant.

The cyclonic conditions are considered in the mooring study of the platform, which is explained in detail in Section 4.4.

2.3.4 Operational Conditions

Current

The first assumption made regarding the environment is that the pipe faces a constant current over time, as the time scale of a change in current is very large (hours) compared to the time of the simulation. This assumption is very common as explained in DNV-GL Recommended Practice on Environmental Conditions and Environmental Loads [3]. Regarding its direction and amplitude, there is a lack of precise data near the site of the platform. However, IFREMER[2] conducted a survey campaign in Aldabra, an atoll located in the South West of the Indian Ocean, at the North of Madagascar[4], subject to the same global current: the South Equatorial current of the Indian Ocean as shown in Figure 2.5 marked under a blue rectangle. The maximum amplitude of the current has been decided to be at 0.4 m/s for this study.

Waves

The wave data used for the study comes from the CEREMA[3]. The waves have been observed during 17 years near the zone of the platform, and the observations are summed up in the Figure 2.6, where the percentage of occurrence of different sea states are plot, characterized with the significant wave height (H_{m0}) and the peak wave period (T_p). The Le port's wave surveys in Figure 2.6 show that the vast majority (95%) swells is of low amplitude, significant height H_{m0} less than 1.64m. The highest 5% of amplitudes are due to southern and cyclonic swells. This can go up to a significant height H_{m0}=6m.
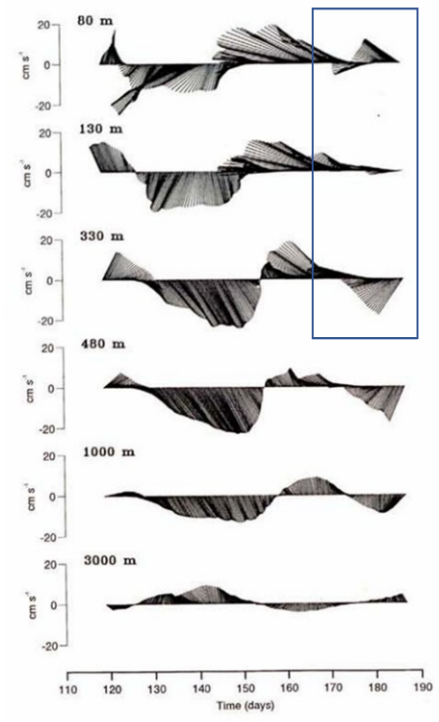
Figure 2.5: Current reading taken off the coast of Aldabran Atoll , north of Madagascar

---

[2] French research institute for the exploitation of the sea

[3]Cerema - Center for studies and expertise on risks, the environment, mobility and planning
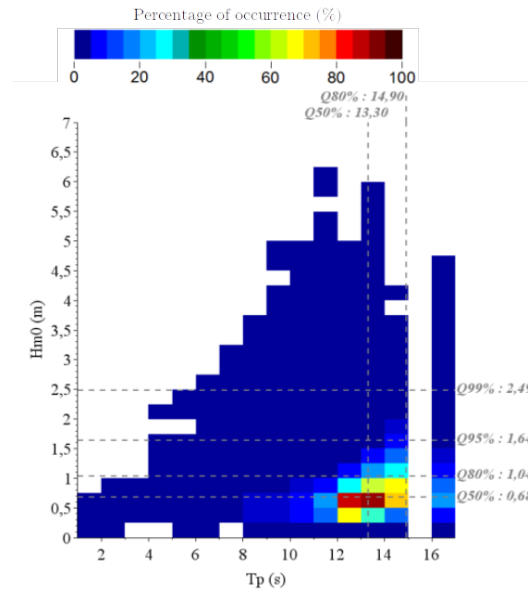
Figure 2.6: Le Port Houlograph Records over 17 Years

The wave conditions used in the study are thus, in terms of significant wave height and peak period:

- Operational : $H_{m0} = 3m$, $T_p = 13s$

- Cyclonic : $H_{m0} = 6m$, $T_p = 14s$

Wind

The wind speed around the city of Le Port is considered from 25 m/s to 70 m/s from operational conditions to cyclonic conditions. Therefore, the wind speed for operational condition is 25 m/s and the cyclonic condition to be 70 m/s.

2.4 Hydrodynamic coefficients

The environmental forces are calculated using Morison's Equation, thus the influence of the drag (C_D) and added mass (C_M) coefficients is crucial. Moreover, the Strouhal number (St), governing the frequency of vortex shedding, shall be known to avoid lock-in. These coefficients depend mainly on the shape of the pipe and the Reynolds Number of the flow, and are usually determined via experimentation and/or CFD[4] studies. However, as the project is at its initial phase, the determination of the coefficients is based on the crosses of empirical values or formulas found in different existing experimental studies.

---

[4]Computational Fluid Dynamics

Drag coefficient

To determine the drag coefficients, two references are used for determining the drag coefficient. Two case studies with a similar shape and Reynolds's number are described below. The geometry of the structures referred in the case studies are described in Annexure A:

- DNV-RP-C205 Recommended Practices[3] have two cases which are most similar to the proposed design of CWP :

  - the six-strand wire, C_D found is in the range between 1.5 and 1.8
  - The diamond with rounded corners, C_D found equal to 1.5

- Hoerner-Fluid-Dynamic-Drag book[5] details two study cases whose geometry can be referred :

  - the rough cylinder, which has a C_D of 1.17
  - the inclined square, which has a C_D of 1.55

From the above cases where it has been decided to take a value for the drag coefficient of 1.5.

Added Mass Coefficient

The determination of added mass coefficient is carried out similarly. DNV-GL Recommended Practice: Environmental Conditions and Environmental Loads[3] practices specifies the coefficient for the circular cylinder with fins (analogy with stiffeners) is 0.87 therefore this value is chosen for the pipe hydrodynamic study. The geometry description can be found also in Annexure A.

Strouhal Number

The Strouhal Number can be obtained as a function of Reynolds number as follows from [6] :

$$S_t = 0.213 - 0.0248 \left(log \left(\frac{R_e}{1300} \right)^2 \right) + 0.0095 \left(log \left(\frac{Re}{1300} \right)^3 \right) \tag{2.1}$$

where, R_e is Reynolds's Number

As the R_e is a function of the water viscosity, which depends on the temperature, the Strouhal number is a function of the temperature. For a range of temperatures between 5 and 25 degrees, St is between 0.33 and 0.38. The link between the Strouhal number and the vortex shedding frequency f_v is the following :

$$f_v = \frac{S_t U}{L} \tag{2.2}$$

where U is the water velocity and L the characteristic length, here the diameter. Thus, the vortex shedding frequencies are between 0.027 and 0.03 Hz.

The further detailed work has to be carried out via CFD and Tank Test to determine the Vortex Induced Vibrations in the pipe and to verify if the vortex induced frequency matches with the analytical calculations.

Chapter 3

Design loads

In order to determine the behaviour of the pipe and analyse the global behaviour of cold water pipe, it is necessary to establish the design loads subjected on the cold water pipe. For this purpose, an in-house calculation code named cPendulum is being developed which is used to determine the movements of the pipe as a function of the environmental conditions. In Figure 3.1 various design loads are summarised.
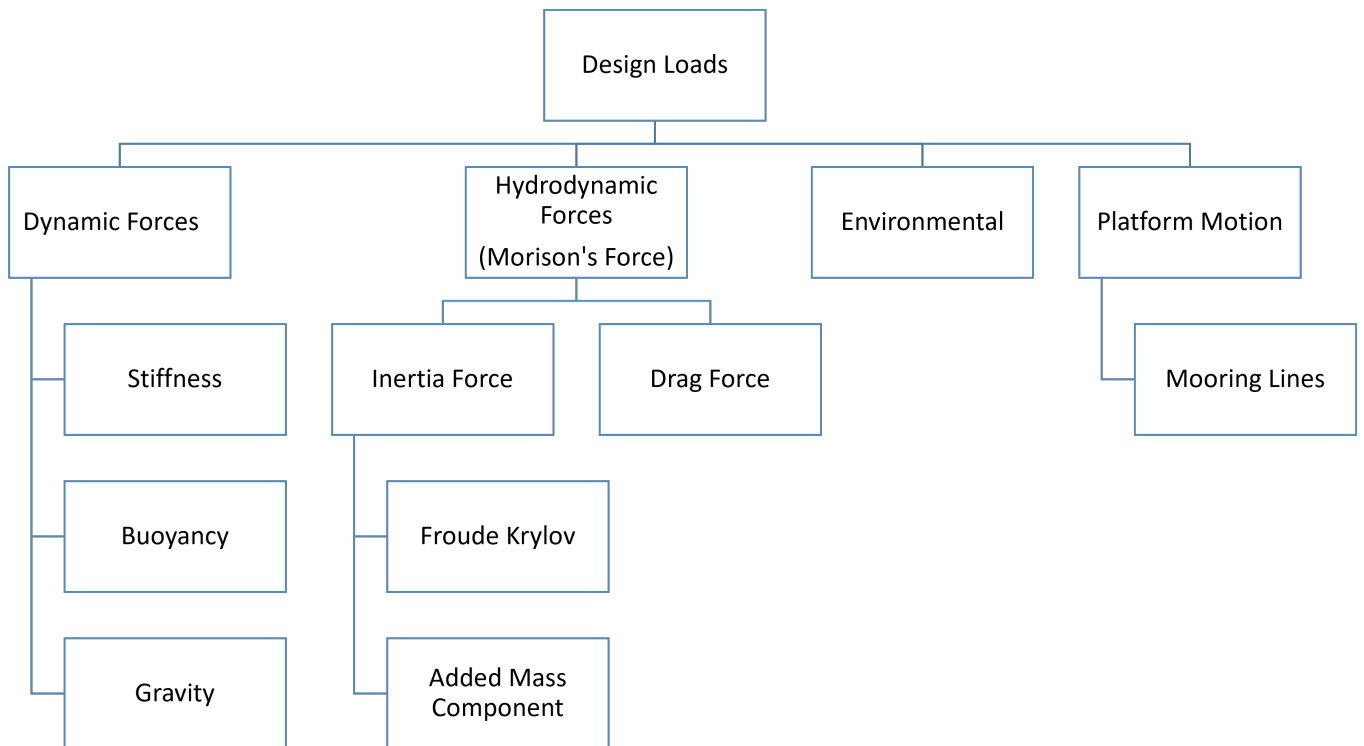
Figure 3.1: Design Loads used with cPendulum

3.0.1 cPendulum code

The cPendulum code has been developed by team of Deeprun and energy lab where, I participated to develop and improve the aspects related to hydrodynamics.The code is used to know precisely the behavior of the pipe at the global scale. It is based on a model of 1000 masses linked by pendulums and aims to model the movements of the CWP represented in yellow in the Figure 3.2.
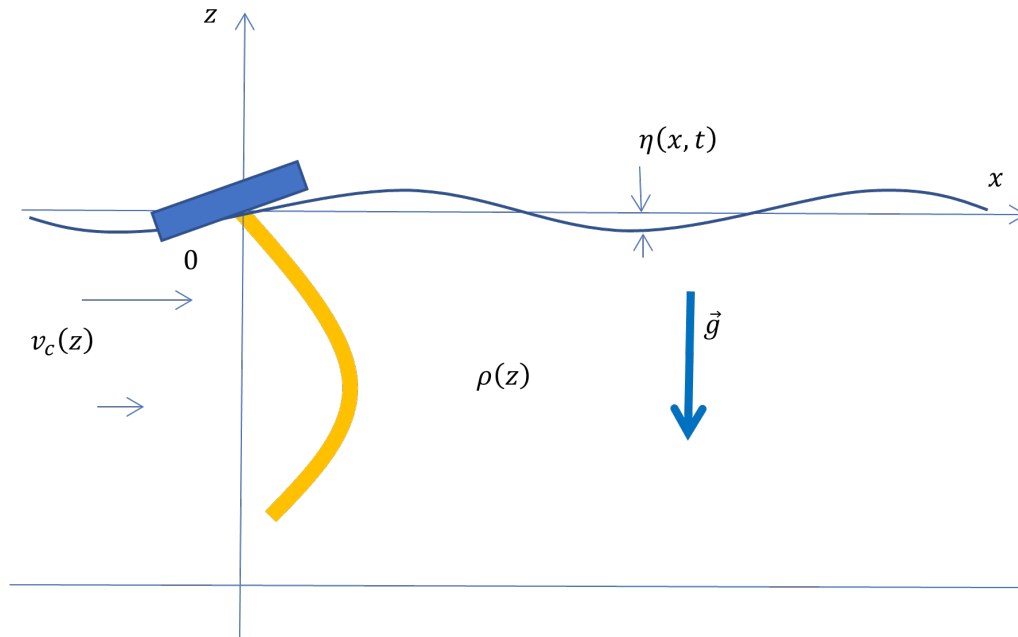
Figure 3.2: Plant schematic view

CWP is modelled and discretised as a series of masses attached to each other. This mass sequence constitutes a multiple pendulum, connected to a surface platform at its upper end and left free at it's lower end. This system is excited by its environment represented by two major components:

- The movements of the platform

- The velocity of the water particles due to current and waves

Summary of forces

All the external forces applied to the system are summarized below:

- Gravity and buoyancy

- Elastic restoring moment which characterizes the stiffness of the connection between two modules.

- Morison forces due to the interaction between the CWP and the moving fluid around it. These forces are divided into the drag force, proportional to the speed and the inertia force proportional to the acceleration.

3.1 Environmental Forces

The main theory used in cPendulum is linear wave theory for simulations and analysis. The work focuses on first order waves, in addition to steady current and the platform amplitude that occurs with them.

3.1.1 Motion of the water particles

Design and analysis of CWP should include the effects of combined wave and current forces. Therefore, the horizontal velocity of the water particles is calculated as the sum of the current speed and the swell velocity:

$$\nu_c = \nu_{current} + \nu_{wave} \tag{3.1}$$

Regular Waves

The regular waves exist only theoretically or created in laboratory which consists of sets of waves with same height and length as each other. Regular waves are shaped like a propagate sine wave which moves along the surface of the water. These waves are periodic in nature which has a consistent frequency and period of occurrence. The table summarises the notation explained in Offshore Hydromechanics[7] that is used to describe the characteristics of regular wave.
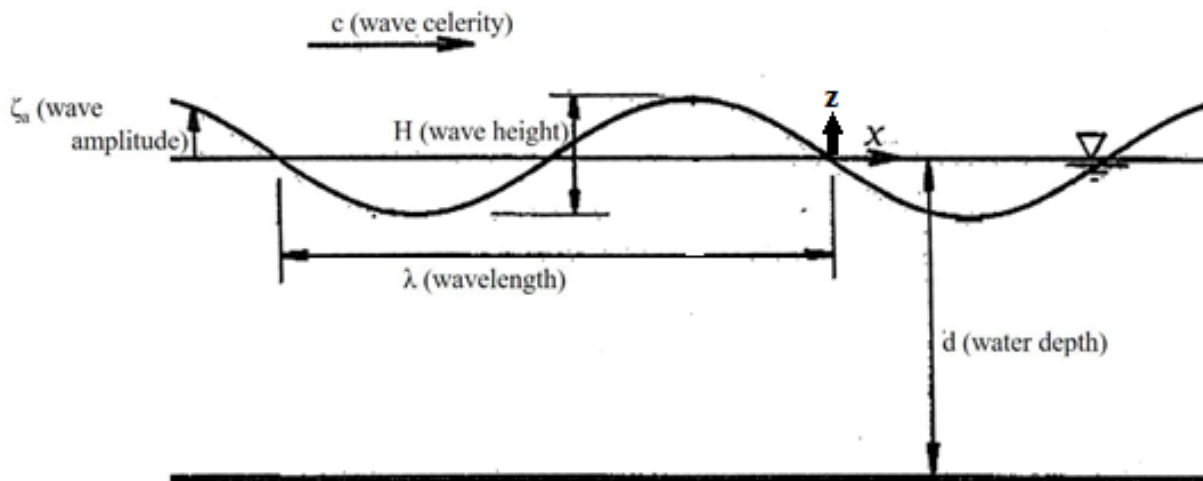
Figure 3.3: Regular Waves

The number of cycles that occur over a unit length is known as wave number whose expression is

$$k = \frac{2\pi}{\lambda} \tag{3.2}$$

The equation for water surface elevation accounts for the point at which wave is measured along

Table 3.1: Characteristics of Waves

ζ_0	the wave amplitude from mean level to crest or trough
H	wave height (twice the wave amplitude)
λ	Wave length (distance from crest or trough to the next)
c	Wave celerity
T	Wave period (time interval between successive crests or toughs passing a fixed point)

with change in space and time to give:

$$\zeta(x,t) = \zeta_0 sin(kx - \omega t + \epsilon) \tag{3.3}$$

- ζ_0 is wave amplitude

- ω is circular wave frequency

- k is wave number

- ϵ is random phase angle

The water depth of the site is sufficiently high to consider deep water conditions. In these conditions, the linear swell theory gives the following trajectory for the water particles:

[Source: Groen and Dorrestein, 1958]
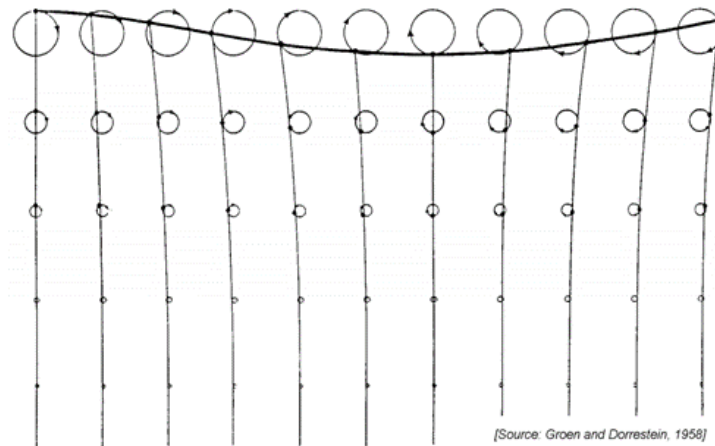
Figure 3.4: Water Particles Trajectory

The wave length of the swell is:

$$\lambda = \frac{gT^2}{2\pi} \tag{3.4}$$

The wave celerity defines the speed of the wave traveling over the water surface and in deep water the wave celerity is given as:

$$c = \frac{g}{\omega} \tag{3.5}$$

The horizontal and vertical velocities of the water particles are:

$$\nu_{wave,x}(x,z,t) = \frac{\pi H}{T} exp(\frac{2\pi z}{\lambda}) sin\left(2\pi\left(\frac{x}{\lambda} - \frac{t}{T}\right)\right) \tag{3.6}$$

$$\nu_{wave,z}(x,z,t) = \frac{\pi H}{T} exp(\frac{2\pi z}{\lambda}) cos\left(2\pi\left(\frac{x}{\lambda} - \frac{t}{T}\right)\right) \tag{3.7}$$

and the horizontal and vertical accelerations of the water particles are:

$$a_{wave,x}(x,z,t) = \frac{2\pi^2 H}{T} exp(\frac{2\pi z}{\lambda}) cos\left(2\pi\left(\frac{x}{\lambda} - \frac{t}{T}\right)\right) \tag{3.8}$$

$$a_{wave,z}(x,z,t) = -\frac{2\pi^2 H}{T} exp(\frac{2\pi z}{\lambda}) sin\left(2\pi\left(\frac{x}{\lambda} - \frac{t}{T}\right)\right) \tag{3.9}$$

Irregular Waves

The waves in the sea are generally 'irregular' which are chaotic or random. Any two waves in the sea do not have the same height or length. The behaviour of regular waves with the principal of linear superposition, where the set of appropriate regular waves are used to create a new wave set/shape for modelling irregular waves[7]. The time history of wave surface elevation is expressed as:

$$\zeta(t) = \sum_{n=1}^{\infty} \zeta_{i0} sin(k_i x - \omega_i t + \epsilon_i) \tag{3.10}$$

where

- ζ_{i0} is wave amplitude
- ω_i is circular wave frequency
- k_i is wave number
- ϵ_i is phase of the wave component i

Wave Energy Spectrum

For Irregular Sea states, wave kinematics is generated based on an appropriate wave spectrum. The wave component (each sinusoidal wave) which makes an irregular wave pattern, is quantified in terms of wave amplitude energy density spectrum, also known as wave energy spectrum[8]. The Figure 3.5 represents the spectral ordinate value on the vertical axis. The area under the curve equals the energy of that frequency component wave and the spectral ordinate for each frequency is

$$S_\varsigma(\omega_i) = \frac{\varsigma_{i0}^2}{2\Delta\omega} \tag{3.11}$$

where: $\Delta\omega$ is the bandwith of the frequency. Now an random phase in being introduced. In reality, the number of sine wave components are infinite. However, a limited number is used as the small ordinate values can be ignored. From the changing, the spectral ordinate equation gives the wave amplitude for each frequency component:

$$\varsigma_{i0} = 2\sqrt{S_\varsigma(\omega).\Delta\omega} \tag{3.12}$$

The amplitude can be determined knowing that the area under the associated segments of the spectrum $S_{\sigma\omega} \times \Delta\omega$ is equal to variance of the wave component.
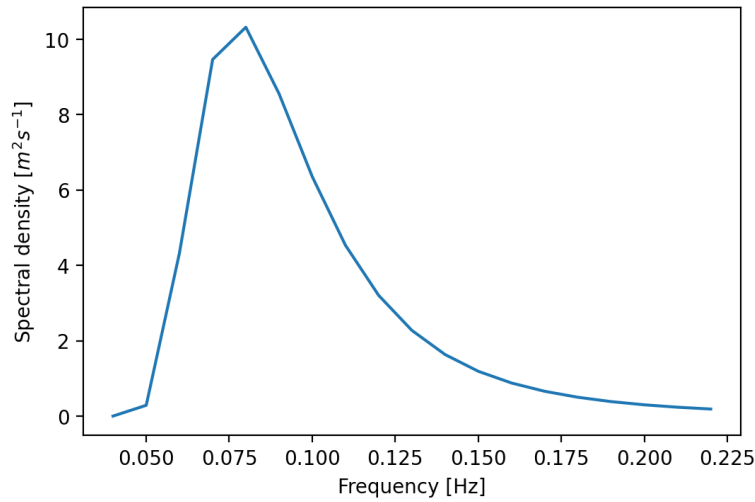
Figure 3.5: Spectral Density Curve

The steps to implement the irregular waves in cPendulum are represented in Figure 3.6. Once the wave spectrum is defined, it is imported in Ansys AQWA as User defined wave spectrum.
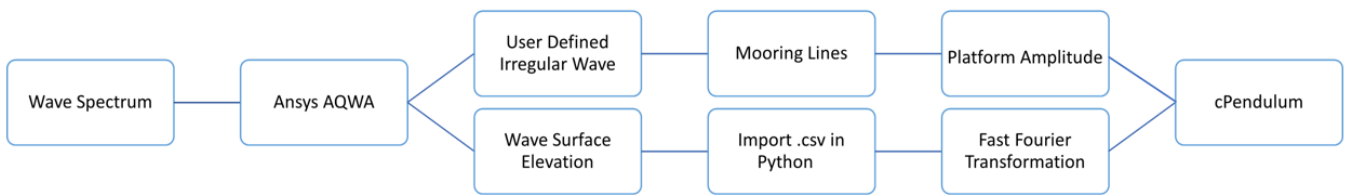
Figure 3.6: Process for Implementation of Irregular Waves

Firstly, Ansys AQWA uses this wave spectrum to generate irregular waves that are used for determining the mooring system and platform amplitude.

Secondly, Ansys AQWA captures the wave surface elevation which is created by software from the user-defined wave spectra. The Figure 3.7 shows the wave surface elevation obtained from Ansys AQWA. Once the wave surface elevation is captured, it is exported as *.csv* file which is used in cPendulum for simulating the motion of pipe under the same irregular wave.
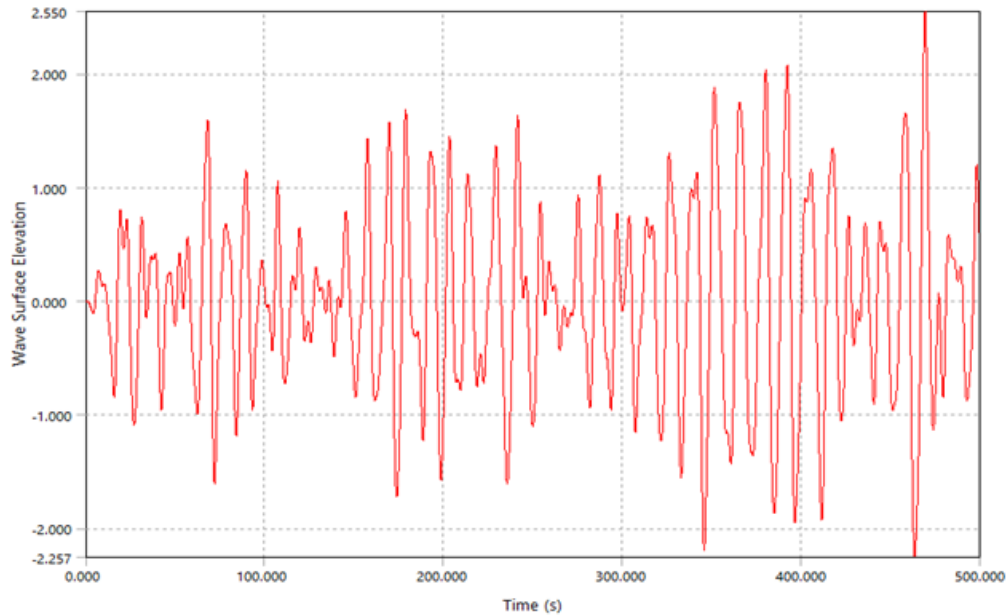
Figure 3.7: Wave Surface Elevation from Ansys AQWA

Fourier transformation

Furthermore, to implement the wave surface elevation captured from Ansys AQWA in cPendulum, the signal is decomposed into finite number of (co)sine-waves using Fourier Transformations. The Fast Fourier transformation is then used to gain a statical description of the original wave record. Thus, reverse engineering from a given wave record to ISSC spectrum and from this spectrum back to a simulated wave record[8]. The results captured using FFT[1] will enable to simulate accurately a 'real' sea state with parameters that will be implemented in cPendulum code and platform amplitude.This flow process explained above is summarised in Figure 3.6.

The Fourier transformation enables to find at a given position x, any wave shapes which are the sum of regular waves, different frequencies, amplitudes, and phases. The idea behind using the Fourier transformation is to figure out the set of frequencies, amplitudes, and phases that make up the irregular wave[9]. Once the irregular wave train is created by combining many components of different frequencies, the Fourier transformation identities the amplitude and phase angle associated with each frequency component in wave. Applying the FFT will produce an exact amplitude and phase of those sine waves, with no errors. The Figure 3.8 below represents the irregular wave which is re-traced using FFT.

---

[1]Fast Fourier Transform
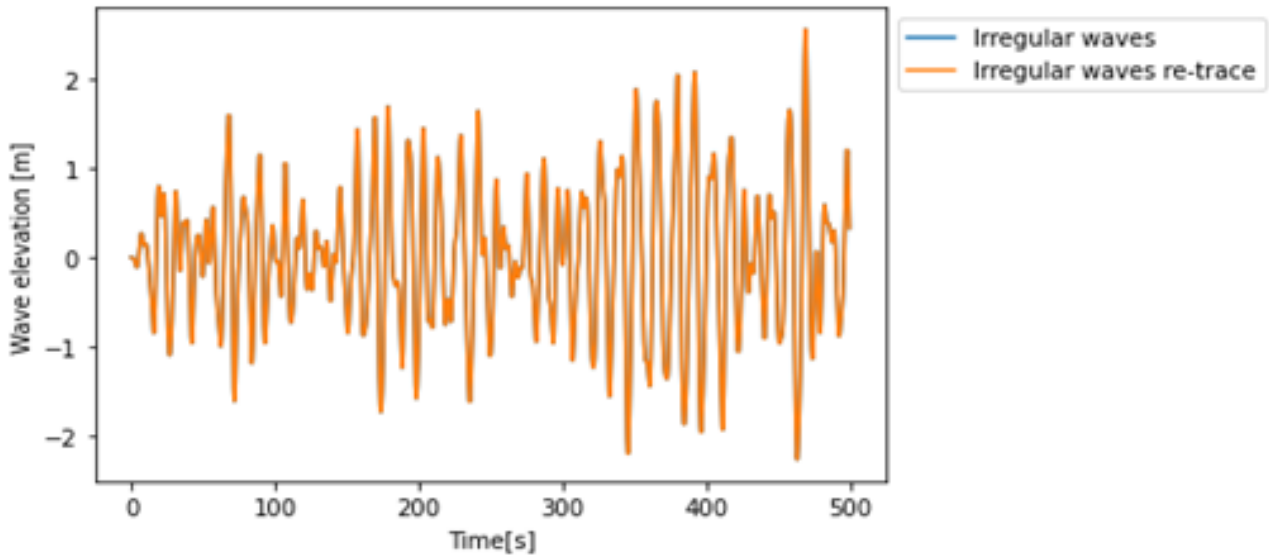
Figure 3.8: Retracing irregular Waves

Now the amplitude, phase, and frequency of the irregular wave is captured, it is used in cPendulum to apply these irregular waves to CWP.

3.1.2 Current

The global behaviour of CWP is influenced by the current forces which will be directly applied to the CWP as well as influencing the design of mooring lines which is impacted and will have effect on the total system.

The variation in current velocity with changing depth depends upon the oceanic conditions at that particular location, density distribution, and the flow of water in or out of the area. In this thesis, the current is considered constant over time as the time scale of a change in current is very large (hours) compared to the time of the simulation and depends only on the water depth d and is purely horizontal. The profile used to calculate the current is the shear current profile shown in Figure 3.9 which is created positively for descent vertical axis.

$$\nu_{current} = \nu_{max} cos\left(-\frac{5\pi z}{d}\right) e^{z/d} \tag{3.13}$$

where,

- ν_{max} is maximum current speed

- d is water depth

- z is vertical position from water level
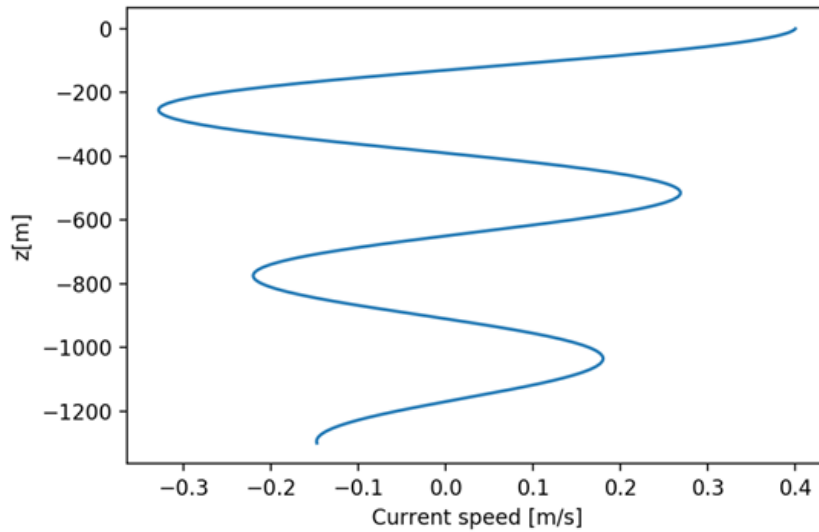
Figure 3.9: Current Speed

3.2   Morison's Forces

Morison forces, which are the interaction between the moving fluid (water) around the structure and the pipe. For calculating the wave loads on pipe, the Morison's forces are divided into two terms: one is related to water particle acceleration, the fluid inertia force, and one is related to water particle velocity, the drag force.

Drag Force

Drag force is a non-conservative force as it dissipates the energy of the system. It is expressed as:

$$\vec{F_{Tk}} = \frac{1}{2}\rho_k C_{D,k} S_k \left|\vec{v_k}\right| \vec{v_k} \tag{3.14}$$

where

- ρ_k is density of water

- $C_{D,k}$ is Drag Coefficient of module k

- S_k is Surface Area of module k

- $\vec{v_{r_k}}$ is the fluid velocity relative to the body

Inertia Force

Inertia Force is a conservative force, so it derives from a potential. The inertia force is a sum of two terms:

- Added Mass Component, proportional to the acceleration of the body:

$$\vec{F}_{am_k} = \rho_k \pi L_k R_k^2 C_{a,k} \vec{a_k} \tag{3.15}$$

where,

  - ρ_k density of water around module k
  - L_k Length of the module k
  - R_k radius of the module k
  - $C_{a,k}$ added mass coefficient of module k
  - a_k is the acceleration of module k

- the Froude-Krylov component, proportional to fluid acceleration, which derivates from a potential:

$$\vec{F_{fk_k}} = \rho_k \pi l_2 R_k^k \left(1 + C_{a,k}\right) \left(\left(\dot{v_{c_{x,k}}} cos\theta_k + \dot{v_{c_{z,k}}} sin\theta_k\right) \vec{e_{\theta_k}} + \left(-\dot{v_{c_{z,k}}} cos\theta_k + \dot{v_{c_{x,k}}} sin\theta_k\right) \vec{e_{r_k}}\right) \tag{3.16}$$

where,

  - $\dot{v_{c_{x,k}}}$ horizontal acceleration of free particles
  - $\dot{v_{c_{z,k}}}$ vertical acceleration of free particle
  - $\vec{e_{\theta_k}}$ ortho-radial unit vector
  - $\vec{e_{r_k}}$ radial unit vector

Chapter 4

Motion of the Platform

4.1   Introduction

Offshore floating platform needs a mooring system for maintaining its offset within a particular radius under wind, wave, and current loads. OTEC Platform must be able to maintain its positioning to sustain efficient operation, as well as for safety reasons. The orientation of OTEC platform relative to the environment is critical in its operation and therefore a mooring system should be able to provide enough restoring force to keep the platform within a certain limit of offset in various degrees of freedoms.

A mooring system for an offshore floating platform is designed against the overload of any mooring line. Overload is defined as the tension in a line that exceeds the maximum tension including a given safety margin, as outlined in DNV-GL-E301 Offshore Standard. The governing excitation mechanism for mooring line tension is the top end motion of the line, i.e., the static and dynamic motion of the floater itself. The forces induced on the mooring lines of the vessel are generally much larger than the forces that act directly on the mooring lines. For this, permanent mooring lines are studied.

In this chapter, the principal particulars of platform's hull is defined and then maximum environmental forces are calculated which are subjected to the platform. After that, the eigen frequencies of motion of the platform are studied, and as the eigen frequency is similar to the wave frequency, the damping is determined because it governs the motion. Once the mooring lines and the damping of the platform is defined, an Ansys AQWA time domain simulation is performed to calculate the motion of the platform.

Since the platform needs to resist the violent tropical cyclonic condition, the Mooring System needs to be designed such that it does not break in cyclonic conditions ensuring proper stationkeeping.

4.2   Platform Definition

The OTEC platforms used for RUNETM have been referred to the parent hull of an existing French Project, from which the principal parameters are deduced from. However, since the motion of platform have a strong influence on the motion of the CWP, the hull used in this thesis is just a case study and by all means the CWP could be deployed on other type of platform if necessary. The decided principal particulars are shown in Figure 4.1.

(a) Front View

(b) Side View
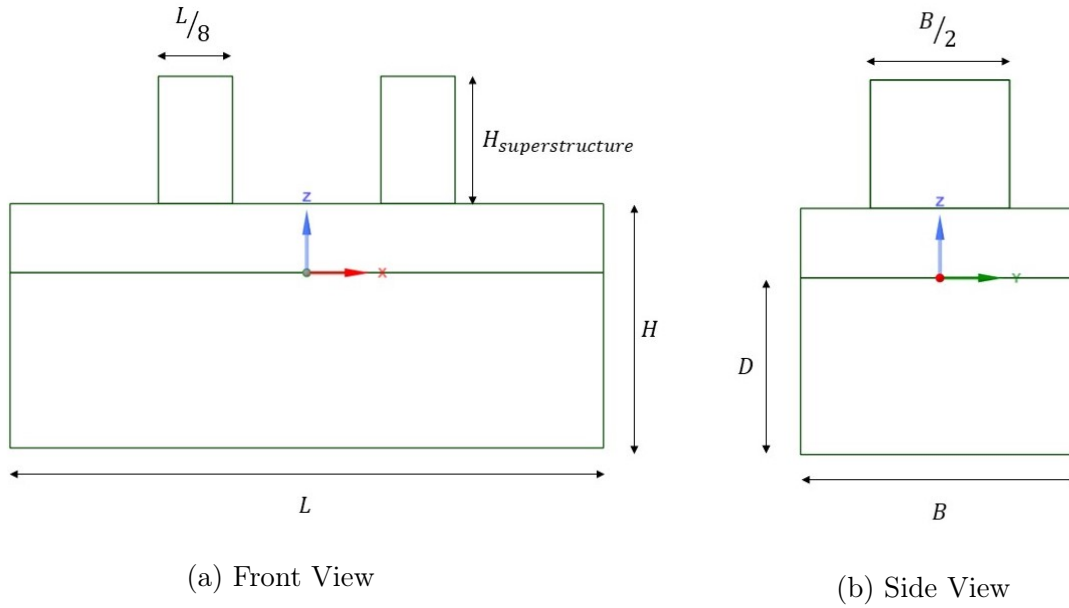
Figure 4.1: Platform Definition

- Length(L):56[m]

- Breadth(B):26[m]

- Depth(D):23[m]

- Draft(T):16.5[m]

- H$_{\text{Superstructures}}$:12[m]

4.3   Environmental Forces

The external forces applied through the environment to the platform will be calculated in two steps. The first one is the evaluation of the screen area and the second one is the evaluation of the pressure. The surface area that is exposed to air and water will have influence on the force that will exert on the platform. Therefore, the force will be calculated as the product of the screens by the pressure:

$$F = A \times P = \frac{1}{2} \rho C_D A V^2 \tag{4.1}$$

where:

- ρ is density of atmosphere

- C_D is drag coefficient

- A is screen area

- V is atmospheric velocity

4.3.1 Screens

A solid screen, in the wind or in the wave + current velocity field $\vec{V}$, is the result of its volume projected on a plane perpendicular to the velocity $\vec{V}$. The wetted surface area is considered by the area which is exposed to swell and current on the platform in contact with the water when a wave arrives on the platform . Therefore, the wave amplitude should be added to the draft for determining the wetted surface area. Whereas the surface area exposed to air considers the height of superstructure. The Figure 4.2 shows the platform screen exposed to wind and water.
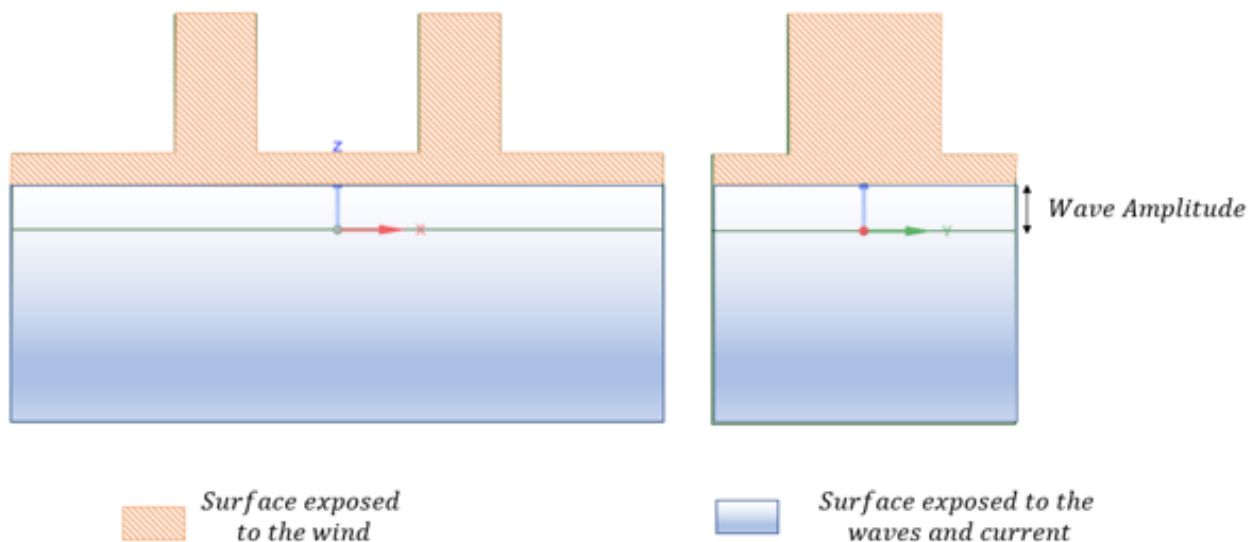
Figure 4.2: Platform Screens

Screen exposure to Highest Environmental Forces

Application of environmental force to the screen either in x-axis or y-axis will depend on the worst conditions the platform may experience. To analyse which screen will receive the most environmental force, determination of the angle which will have the most impact on the platform from environmental forces is important for stationkeeping of the platform.

All environmental loads are assumed to be acting in the same direction. As the platform is rectangular and symmetric, where the 0° is along the positive x-axis and 90° is along the positive y-axis. The angle α from 0°to 90° on symmetric platform is studied as shown in Figure 4.3. In Figure 4.3 (a)and(b) is $\alpha_a \in 0, 45$ and $\alpha_b \in 45, 90$ respectively. The angle α is arctan(L/B) which equals to 66°.Now the angle α_a and α_b needs to be concatenated to discretize into smaller angles between 0°to 90°.

(a) Angle of Attack between 0° to 45°   (b) Angle of Attack between 45° to 90°
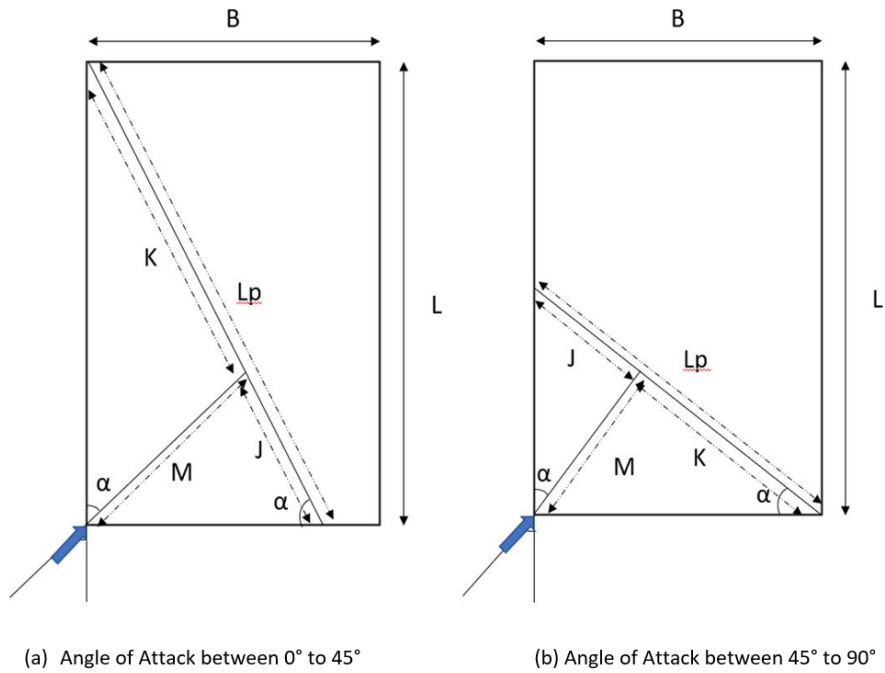
Figure 4.3: Worst Projected Length of Environmental Conditions between 0°to 90°

$$L_{p_x} = B \left[cos\alpha + \frac{sin^2\alpha}{cos\alpha} \right]$$
$$L_{p_y} = L \left[sin\alpha + \frac{cos^2\alpha}{sin\alpha} \right] = L\frac{1}{sin\alpha}$$

(4.2)

The total projected length is $L_p = L_{p_x} + L_{p_y}$.The Figure 4.4 shows that Lp is higher at 66 degrees. Furthermore, to determine the drag force, the drag coefficient needs to be assigned to the platform at various angles. The relationship between drag coefficient and length are shown in Figure 4.4 and can be decided that at the angle 90°, the drag coefficient is 1.5 with drag coefficient to be 1.15 at angle of 45 °.
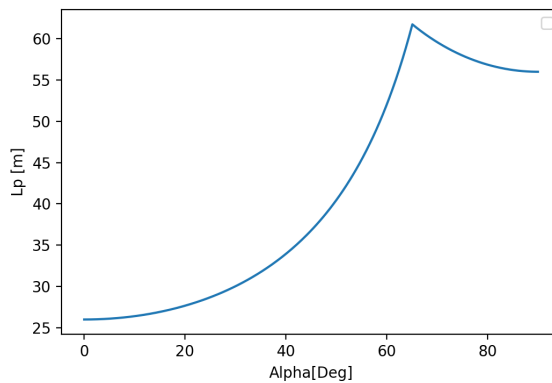
Figure 4.4: Alpha vs Lp

.

$$F_{water}(\alpha) = \frac{1}{2}\rho C_D(\alpha)_\alpha S_D(\alpha)V^2 \tag{4.3}$$

with

$$S_D = (Draft + \varsigma)L_p$$

Now, since drag coefficient is established, force needs to be determined at various angles between 0°to 90° for capturing the angle at which the most environmental force is experienced which is calculated from equation 4.3. From Figure 4.5, it can be seen that the force as a function of the angle is maximum at $\alpha = 90$ in with water, which will be similarly true for wind. For the further mooring system analysis for partial safety factors check and time domain response of platform amplitude will be done at environmental force being projected at y-axis in Ansys AQWA.

(a) Alpha vs Drag Coefficient   (b) Alpha vs Force[N]
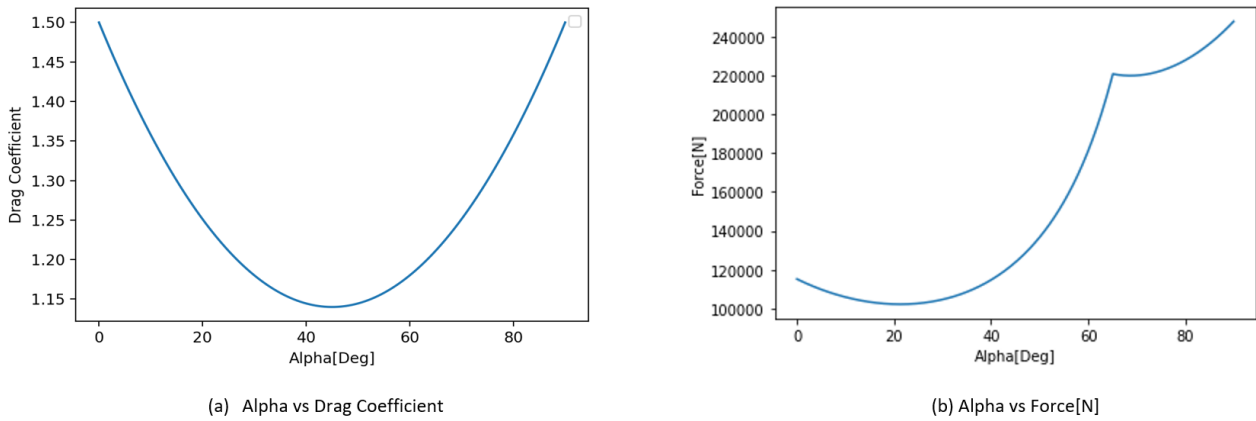
Figure 4.5: Drag Coefficient and Drag Force as a function of environmental angle of incidence

The maximum wave height that is followed in this thesis is summarised below:

- The Maximum wave height in operational condition is $H_{max,ope} = 5.61m$

- The Maximum wave height in cyclonic condition is $H_{max,cyc} = 11.2m$

4.3.2   Wind Pressure

The wind pressure needs to be determined to calculate the wind speed applied to the platform. The usual calculation of the wind speed depending on the altitude, knowing the wind at a given altitude is the following:

$$V(z) = V_{max}\left(\frac{z}{z_{max}}\right)^{\frac{1}{7}} \tag{4.4}$$

With $z_{max}=H_{super} + H - D = 19.5m$, the function $y = \left(\frac{z}{z_{max}}\right)^{\frac{1}{7}}$ is plotted on the Figure4.6.
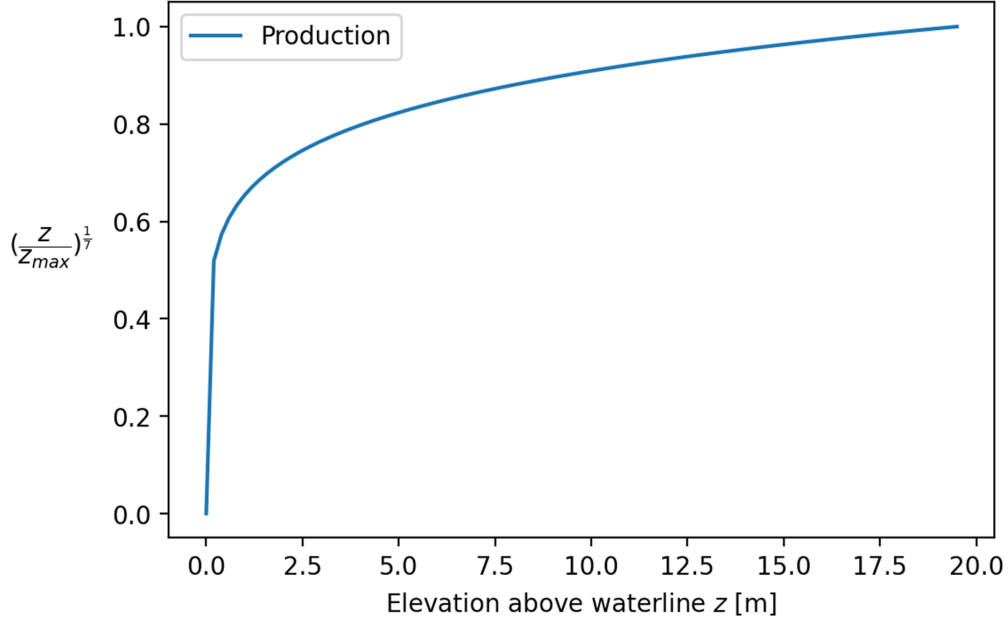
Figure 4.6: Function of wind speed depending on elevation

In the range of elevation above the waterline corresponding to the platform, i.e above $\zeta_{ope} = 2.81m$, this function is close to 1, so as a predesigned approximation, this function can be supposed equal to 1 and thus the wind is supposed constant. This will be conservative. Thus, considering a maximum cyclonic wind speed constant equal to $V_{wind} = 70m.s^{-1}$, the air at the temperature of 25 °C with a density of $\rho_{air} = 1.18kg.m^{-3}$, and a drag coefficient for the platform of 1.5, the wind pressure is then:

$$P_{wind} = \frac{1}{2} \rho_{air} \ C_D \ V_{wind}^2 = 4350.83 \ Pa \tag{4.5}$$

4.3.3   Water Pressure

The pressure is calculated by Morison's Equation Drag Component as follow's :

$$P(z) = \frac{1}{2}\rho_{water} \ C_D \ V^2(z) \tag{4.6}$$

where $V(z) = V_{current}(z) + V_{wave}(z)$
with $V_{current}(z)$ is supposed constant equal to $V_{current} = 0.4 \ m.s^{-1}$
and

$$V_{wave} = \frac{\pi H}{T}e^{\frac{2\pi z}{L}}cos\theta \tag{4.7}$$

where : T is the wave period , equal to $T = 13$ s and L is wavelength , calculated as

$$L = \frac{gT^2}{2\pi} \tag{4.8}$$

The velocity is plotted on Figure 4.7. As the shape of the platform is constant at its height underwater, the pressure is averaged. The average water pressure is : P_{water}=4624.72 Pa
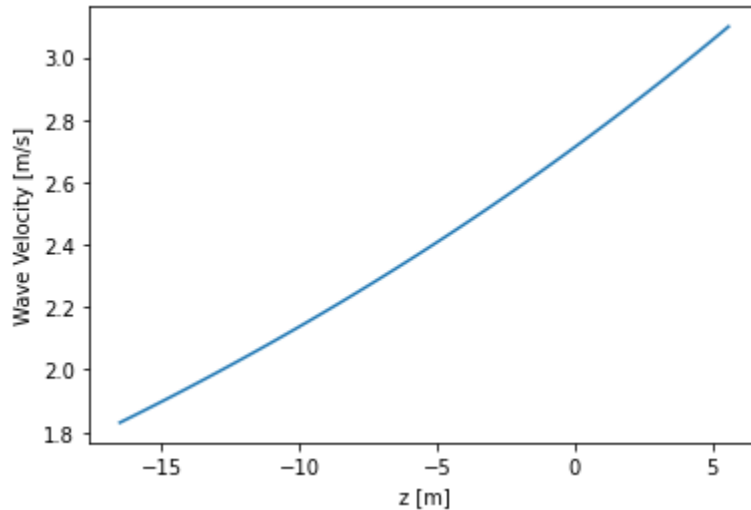
Figure 4.7: Water velocity as a function of height

4.3.4 Total Forces

The platform needs to resist the violent cyclonic condition. A cyclone has the property to create force on a wide range of headings, so the mooring system in section 4.4 is designed to resist to forces coming from both x and y directions.Therefore, the environmental forces subjected to the platform are calculated along x and y directions.

The Environmental Forces are :

$$F_{x,wind} = A_{x,air} \times P_{wind} = 1096.71 \text{kN}$$
$$F_{y,wind} = A_{y,air} \times P_{wind} = 1631.21 kN$$

$$F_{x,water} = A_{x,water} \times P_{water} = 2658.56 kN$$
$$F_{y,water} = A_{y,water} \times P_{water} = 5726.14 kN$$

Therefore, the total environmental forces are:

$$F_{x,env} = F_{x,water} + F_{x,wind} = 3755.28 kN$$
$$F_{y,env} = F_{y,water} + F_{y,wind} = 7357.36 kN$$

With the same direction, co-linear to the x axis is the most extreme case for studying the surge and pitch motions, and colinear to the y axis is the most extreme case for studying the sway and roll motions.

4.4 Mooring System

The mooring system lay-out which is designed for the platform is a catenary system. Catenary system is the oldest and still the most common mooring system. The catenary refers to the

shape that a free hanging line will have under the effect of gravity. The catenary system provides resorting forces through the suspended weight of the mooring lines and its change in configuration arising from vessel motion.

As explained in section 2.3.3 the CWP is not designed to withstand the cyclonic conditions and hence, the pipe will be detached and submerged at a certain depth when a cyclone is announced, but the platform still needs to resist the tropical cyclonic conditions coming from both x and y directions.

However, to satisfy the partial safety factor, the environmental forces are considered colinear to the y axis only for Ansys AQWA simulations as it is the side receiving the highest forces as explained in subsection 4.3.1.

4.4.1   Line Characteristics

The mooring type chosen is a 4-point mooring. These four catenary mooring lines are connected at each corner of the platform and are oriented compared to the x axis with the same angle α. The Figure 4.8 shows the configuration of the platform and its mooring system.
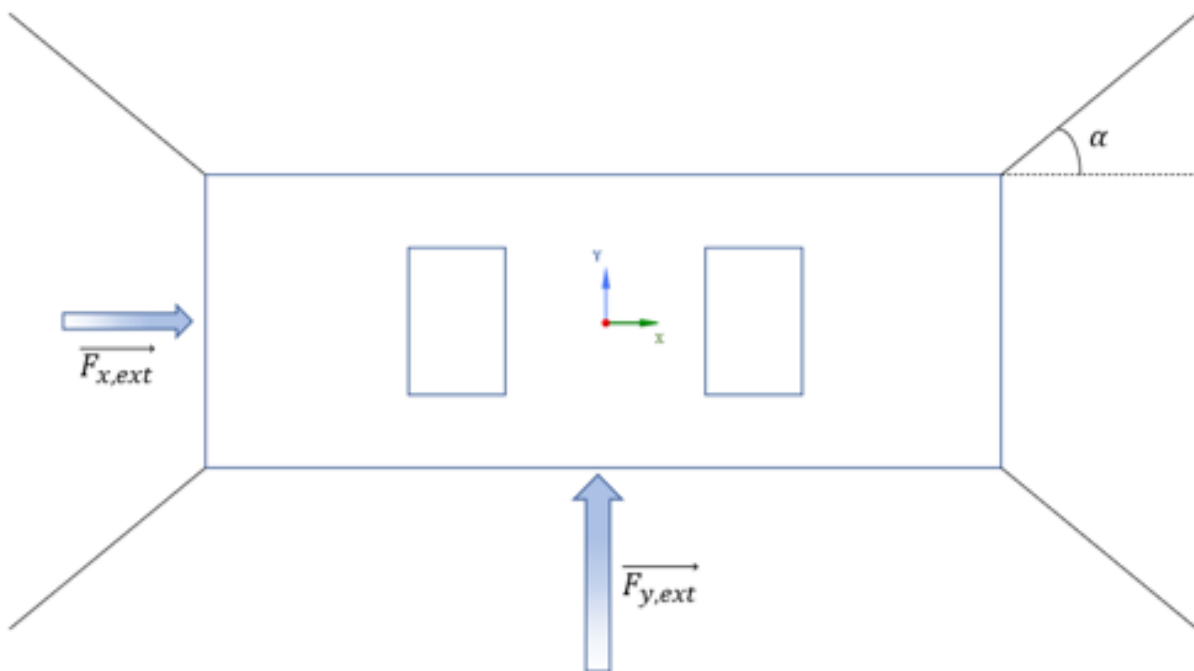
Figure 4.8: Platform and its mooring system

It is a preliminary design, therefore the forces relative to heave, roll, and pitch are not considered, as well as the low frequency response of the platform to the waves.

Looking at the forces submitted to the cable permits to calculate what is the required angle α, and the horizontal tension on the cable T_h. The loads are supported by two bottom cables, represented in the Figure 4.9 which ensures that the load gets distributed. Newton's second law applied to the system gives:

$$2\vec{T_h} + \vec{F_{y,ext}} + \vec{F_{x,ext}} = \vec{0} \tag{4.9}$$

Now projecting on the y axis gives:

$$2\ T_h \sin\alpha = F_{y,ext} \tag{4.10}$$
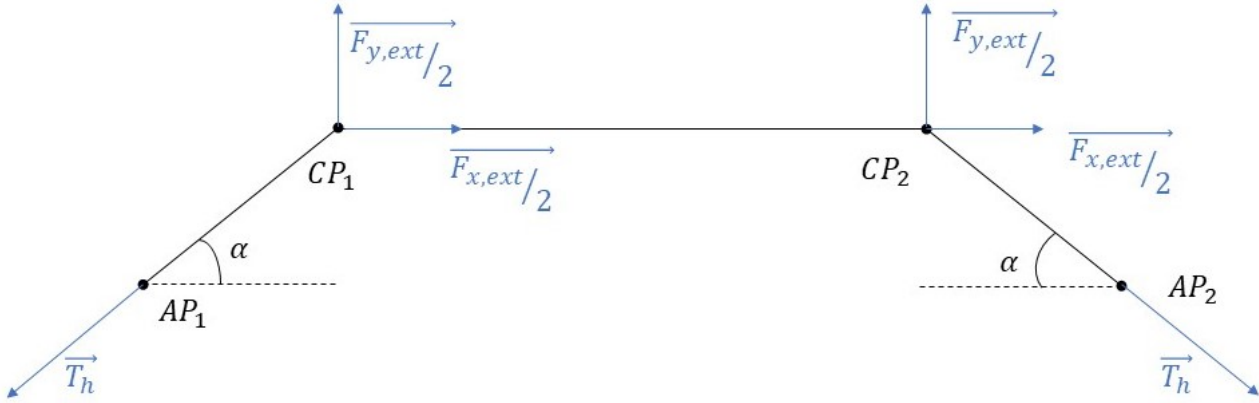
Figure 4.9: Bottom Mooring Cables submitted to the environmental loads

And similarly, considering the environmental forces are coming from the x direction, with the loads supported by two side cables:

$$2\ T_h \cos\alpha = F_{x,ext} \tag{4.11}$$

Squaring and adding the equation(4.10) and equation(4.11) gives :

$$4\ T_h^2 \left(\cos^2\alpha + \sin^2\alpha\right) = F_{x,ext}^2 + F_{y,ext}^2 \tag{4.12}$$

followed by

$$4T_h^2 = F_{x,ext}^2 + F_{y,ext}^2 \tag{4.13}$$

which can be written as:

$$T_h = \frac{1}{2}\sqrt{F_{x,ext}^2 + F_{y,ext}^2} = 4130.15 kN \tag{4.14}$$

and equation(4.10) gives:

$$\alpha = \sin^{-1}\left(\frac{F_{y,ext}}{2T_h}\right) = 64 deg \tag{4.15}$$

The catenary theory gives the suspended length of the mooring line with the following expression:

$$l\ =\ D\sqrt{\frac{2T_h}{g\mu} + 1} \tag{4.16}$$

where μ is the submerged linear mass of the mooring line, and D is the water depth. Thus, to calculate this length, the line characteristics should be determined. First, as the aim is to have a permanent mooring system, the nature of the line chosen is a studless chain. The total tension that will constrain the chain is

$$T = T_h + \mu\ g\ d.$$

This tension also depends on the submerged linear mass of the chain, so a test-based method is used. For the required proof load and submerged linear mass, the diameter of studless chain is elected from *Vicinay Cadenas* company's catalogue[10]. The complete information about the selected mooring cable is given in Annexure B.

The studless chain with a diameter of 140 mm has a linear mass of 341 kg/m, and a proof load of 11186 kN. This proof load is superior to the total tension that can be calculated, and which is equal to 8479 kN, thus this chain fits with our study. With a line composed of a studless chain with a diameter of 140 mm, resulting in a mass of 341 kg/m, the suspended length of the line is:

$$l = D\sqrt{\frac{2T_h}{g\mu} + 1} = 2213.61m \tag{4.17}$$

And the horizontal distance between the connection point CP and the anchor point AP is:

$$L_h = \frac{T_h}{\mu g}\left[\ln\left(\frac{\mu g}{T_h}(D+l) + 1\right)\right] = 1663.06m$$

Thus, the coordinates of the anchoring points are:

$$\begin{pmatrix} \pm L_h \sin\alpha + \frac{L}{2} \\ \pm L_h \cos\alpha + \frac{B}{2} \end{pmatrix} = \begin{pmatrix} \pm 1509.26 \\ \pm 769.05 \end{pmatrix}$$

Marine Growth

According Offshore Standard DNVGL-OS-E301[11], Marine Growth is caused by soft (bacteria, algae, sponges, sea quirts and hydroids) and hard fouling (goose,barnacles, mussels and tubeworms).

Marine growth on the mooring lines is included in the analysis of long term mooring systems for OTEC Platform. The thickness of marine growth depends on the location of installation. The marine growth accounts for increasing the weight of the line and increase in drag coefficient.

The marine growth below 40 m depth is 30 mm with the density of marine growth is set to 1325 kg/m3.

The Mass of Marine Growth is calculated as :

$$M_{growth} = \frac{\pi}{4}D_{nom} + 2\Delta T^2_{growth} - D^2_{nom}\rho_{growth}\mu = 42.5 \ kg/m \tag{4.18}$$

Submerged weight of marine growth:

$$W_{growth} = M_{growth}\left[1 - \frac{\rho_{seawater}}{\rho_{growth}}\right]\frac{9.81}{1000} = 0.09 \ kN/m \tag{4.19}$$

where :

- ρ_{growth} is density of marine growth

- $\rho_{seawater}$ is density of sea water

- D_{nom} is nominal chain diameter

- ΔT_{growth} is Marine growth surface thickness

- μ is 2.0 for chain, 1.0 for wire rope

The Mooring line's drag coefficient needs to be determined considering the marine growth and then inserted as an input in Ansys AQWA for Time domain analysis . Therefore, the increase in the drag coefficient due to marine growth :

$$C_{D_{growth}} = C_D D_{nom} + 2\Delta T_{growth} D_{nom} \tag{4.20}$$

where:

$C_{D_x} = 2.4$ for studless chain $C_{D_z} = 1.15$ for studless chain

The increase in drag coefficient transversely and longitudinally is found to be 3.5 and 1.7 respectively.

4.4.2   Partial safety factors for Mooring Systems

According to DNG-GL-OS-E301[11], the Ultimate Limit States(ULS) corresponds to ensure that the individual mooring lines have adequate strength to withstand the load effect imposed by extreme environmental actions.

The Accidental Limit States(ALS) is to ensure that the mooring system has adequate capacity to withstand the failure of one mooring line due to unknown reasons. According to DNG-GL-OS-E301[11] the Ultimate Limit States (ULS) correspond to the maximum load-carrying resistance. In addition, it should be mentioned that the Fatigue Limit Sates(FTS), which corresponds to failure due to the effect of cycling loading is a very relevant limit state for the design of mooring systems. However, as the project is at a preliminary state, fatigue is not discussed in this thesis and hence will not be further discussed.

The work focuses on finding the partial safety factors as they account for the diversity of the effect of uncertainties of loads and material on reliability. According to DNG-GL-OS-E301[11] to the mooring line components should be manufactured with a high standard of quality control, which need the Partial safety factors and premises to be studied for ULS and ALS .

Partial safety factors and premises

Consequence classes

Two consequence classes are introduced in the ULS[1] and ALS[2] are defined as:

---

[1]Ultimate Limit States
[2]Accidental Limit States

- Class 1 : where mooring system failure is unlikely to lead to unacceptable consequences such as loss of life, collision with an adjacent platform, uncontrolled outflow of oil or gas, capsize or sinking

- Class 2 : where mooring system failure may well lead to unacceptable consequences of these types.

The following two partial safety factors are applicable for studless chain, steel wire ropes and synthetic fibre ropes. As the chosen mooring line is Studless Chain, the partial safety factors are ULS and ALS are characterised.

Partial safety factors for the ULS

The design equation for the ULS is given by:

$$S_c - T_{c-mean}\gamma_{mean} - T_{c-dyn}\gamma_{dyn} \geq 0 \qquad (4.21)$$

where :

- γ_{mean} is Partial Safety Factor on mean tension

- γ_{dyn} is Partial Safety Factor om dynamic tension

- S_c is characteristic strength

- T_{c-mean} is Mean Tension

- T_{c-dyn} is Dynamic Tension

The Table 4.1 shows the partial safety factors on mean tension(γ_{mean}) and partial safety factor on dynamic tension(γ_{dyn}) for ULS and ALS .

Table 4.1: Partial safety factor for ULS and ALS

Partial Safety Factor for ULS			
Consequence Class	Type of Analysis of Wave Frequency tension	Partial Safety factor on Mean Tension	Partial Safety factor on Dynamic Tension
1	Dynamic	1.10	1.50
Partial Safety Factor for ALS			
Consequence Class	Type of Analysis of Wave Frequency tension	Partial Safety factor on Mean Tension	Partial Safety factor on Dynamic Tension
1	Dynamic	1.00	1.10

The design equation is conveniently reformulated by introducing a utilization factor, u:

$$u = \frac{T_{c-mean}\gamma_{mean} + T_{c-dyn}\gamma_{dyn}}{S_c} \quad \text{where} \quad u \leq 1 \qquad (4.22)$$

The OTEC platform is categorized in Class 1 of consequence classes and the value of Mean Tension and Dynamic Tension is captured from Ansys Aqwa after doing the dynamic analysis based on Time domain .

4.5   Eigen Periods of Motion

The generalized equation of motion of the platform in waves is:

$$(M + A)\ddot{X} + B\dot{X} + KX = F_{env}$$

With:

$$M = \begin{pmatrix} m & 0 & 0 & 0 & 0 & 0 \\ 0 & m & 0 & 0 & 0 & 0 \\ 0 & 0 & m & 0 & 0 & 0 \\ 0 & 0 & 0 & I_4 & 0 & 0 \\ 0 & 0 & 0 & 0 & I_5 & 0 \\ 0 & 0 & 0 & 0 & 0 & I_6 \end{pmatrix}$$ the inertia matrix, where:

m is the mass of the platform

$I_4 = m\ r_4^2$ where $r_4 \approx 0.35$ B is the roll radius of gyration

$I_5 = m\ r_5^2$ where $r_5 \approx 0.25$ L is the pitch radius of gyration

$I_6 = m\ r_6^2$ where $r_6 \approx 0.25$ L is the yaw radius of gyration

$$A = \begin{pmatrix} a_1 & 0 & 0 & 0 & 0 & 0 \\ 0 & a_2 & 0 & 0 & 0 & 0 \\ 0 & 0 & a_3 & 0 & 0 & 0 \\ 0 & 0 & 0 & a_4 & 0 & 0 \\ 0 & 0 & 0 & 0 & a_5 & 0 \\ 0 & 0 & 0 & 0 & 0 & a_6 \end{pmatrix}$$ is the added inertia matrix

With for first approximations $a_3 \approx m$; $a_4 \approx 0.25\ I_4$ and $a_5 \approx I_5$. Added mass coefficients depend on the frequency, so the rigorously added inertia matrix should be written $A(\omega)$.

$$K = \begin{pmatrix} 0 & 0 & 0 & 0 & 0 & 0 \\ 0 & 0 & 0 & 0 & 0 & 0 \\ 0 & 0 & K_3 & 0 & 0 & 0 \\ 0 & 0 & 0 & K_4 & 0 & 0 \\ 0 & 0 & 0 & 0 & K_5 & 0 \\ 0 & 0 & 0 & 0 & 0 & 0 \end{pmatrix}$$ is the hydrostatic stiffness matrix

where:
$K_3 = \rho g \int_{S_0} ds = \rho g L B$ where S_0 is the waterplane area
$K_4 = \rho g V_0 G M_T$ where V_0 is the immerged volume
GM_T is the transverse metacentric height, that can be calculated as follow:

$$GM_T = \frac{I_{yy}}{V_0} + z_G - z_B$$

where $I_{yy} = \frac{LB^3}{12}$ is the second moment of waterplane area, z_G the vertical position of the center of gravity and z_B the vertical position of the center of buoyancy.

$K_5 = \rho g V_0 GM_L$ where $GM_L = \frac{I_{xx}}{V_0} + z_G - z_B$ with $I_{xx} = \frac{BL^3}{12}$. Each degree of freedom that has a restoring force has an associated natural frequency. So, there is a natural frequency in heave, roll and pitch. These natural frequencies depend on the inertia, added inertia and stiffness:

$$\omega_i = \sqrt{\frac{K_i}{A_i + M_i}}$$

$$T_i = 2\pi \sqrt{\frac{A_i + M_i}{K_i}}$$

Thus, the first approximation of the natural periods of motion are:

For the heave motion: $T_3 = 11.5s \leftrightarrow f_3 = 0.087$ Hz

For the roll motion: $T_4 = 50.4s \leftrightarrow f_4 = 0.02$ Hz

For the pitch motion: $T_5 = 11.2s \leftrightarrow f_5 = 0.089$ Hz

Therefore, there is a similitude between the natural periods of motion in heave and pitch and the wave period. Resonance is expected. As the motion of resonant systems is governed by damping, the damping of the system should be determined

4.6 Damped Dynamics of the Platform under Operational Conditions

DNVGL-RP-C205 Environmental conditions and environmental loads [3] motion damping of large volume structures is due to wave radiation damping, hull skin friction damping, hull eddy making damping, viscous damping of bilge keels and other appendices, and viscous damping from risers and mooring. Wave radiation damping is calculated from the potential theory. Viscous damping effects are usually estimated from simplified hydrodynamic models or from experiments. For simple geometries, Computational Fluid Dynamics (CFD) can be used to assess viscous damping.

The study of damping is carried out with operational conditions which are summarised in Table 4.2

Table 4.2: Operational Environmental Conditions

Operational Conditions	Values
Wave Amplitude	2.81 m
Current Velocity	0.4 m/s
Wind Velocity	25 m/s

First, the wave radiation damping, determined by AQWA, is plotted for heave in the following Figure 4.10.
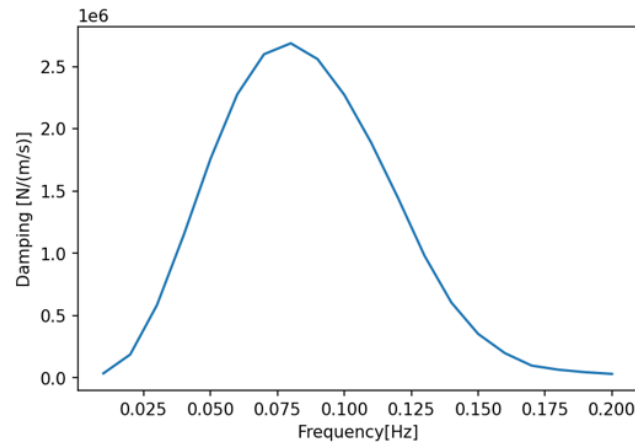
Figure 4.10: Heave Radiation Damping

The RAOs of the platform with wave radiation damping, the only considered damping, are for heave and pitch Figure 4.11.
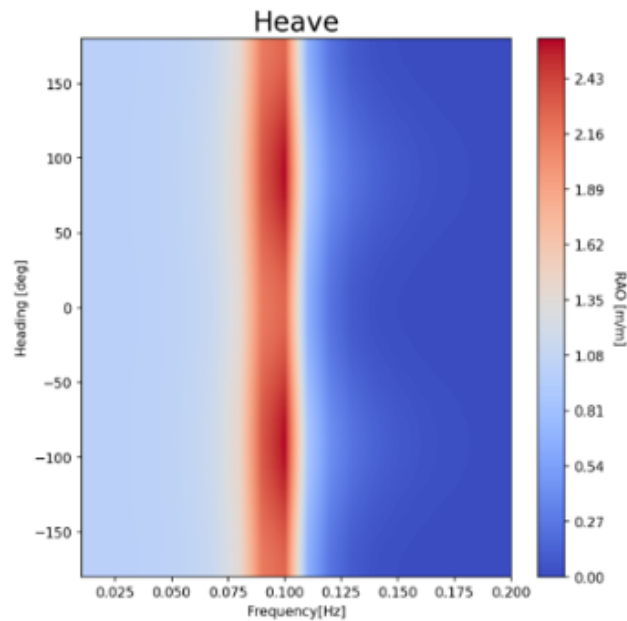

Figure 4.11: Heave RAO of Undamped platform

The values are very high: a vertical motion of 2.5m and a rotation of 20 degrees per meter of wave amplitude.

Thus, a simulation of the dynamics of the platform under operational conditions, where the only damping considered is the wave radiation damping, shows large motions in heave as shown in Figure 4.12.

Then, viscous damping from hull skin friction needs to be determined.

However, this type of data is not available with simple physics, it is calculated after model tests of CFD analysis. As there is not any model test nor CFD calculations made about the
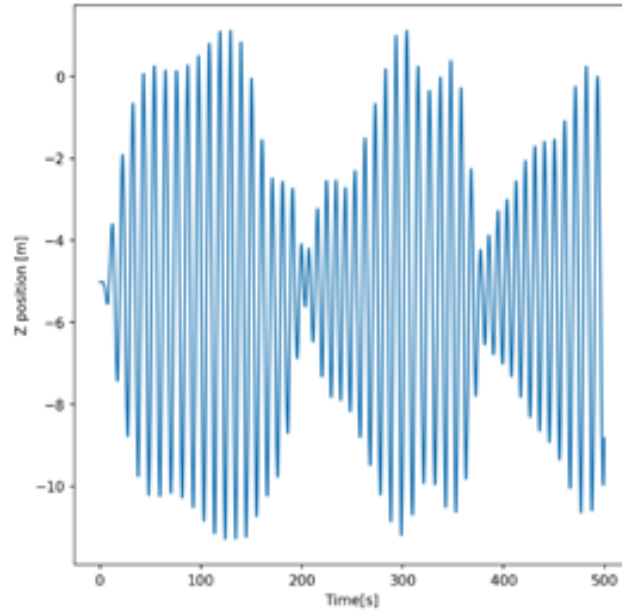
Figure 4.12: Heave Motion of undamped Platform

platform, the viscous damping is then approximated thanks to data of similar size platforms.

4.6.1   Viscous Heave Damping

The formula of the viscous damping heave force is the Morison drag force:

$$F_{D,3} = b_{Q,3}\dot{x}_3\left|\dot{x}_3\right| = \frac{1}{2}\rho C_{D,3}S_3\dot{x}_3\left|\dot{x}_3\right| \tag{4.23}$$

with $\dot{x}_3$being fluid velocity relative to hull .It can be linearized with an equivalent linear damping, and it is related to the quadratic damping with the following formula:

$$b_{Q,3} = \frac{3T_0}{16x_{a,3}}b_{L,3} \tag{4.24}$$

where S_3=$B \times L$ the heave reference area, $b_{L,3}$ is the linearized heave damping, $C_{D,3}$ is the heave linearized drag coefficient, T_3 is the eigen period of heave motion and $x_{a,3}$ the amplitude of heave motion and T_0 natural roll period with ρ being density of water. Thus,

$$b_{L,3} = \frac{8\rho S_3 C_{D,5}x_{a,3}}{3T_3} \tag{4.25}$$

The first approximation of $b_{L,3}$ is given by *Hydrodynamic coefficients for a 3-d uniform flexible barge* [12], for a barge which length is L=120 m, its breadth is B=14 m and draft is D=5.575 m. It is given in Figure 4.13.

First, the heave reference areas of both ships are very close : Platform: $S_{3,platform} = 1456 \ m^2$ Barge: $S_{3,barge} = 1680 \ m^2$. Furthermore, they have a similar shape (box shape), so the assumption that C_D is similar for both ships can be made. Thus, the following equation can be written:

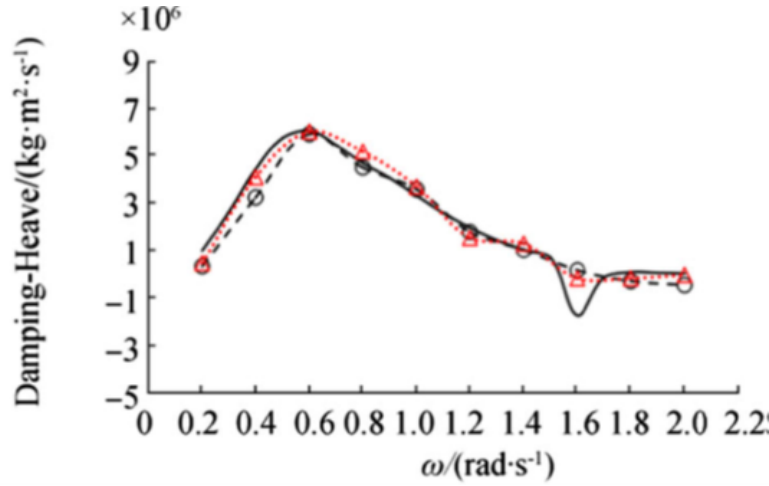$$C_{D,3} = C_{D,3,barge} = C_{D,3,platform}$$

Figure 4.13: Heave Damping for the barge

$$\frac{8\rho S_{3,barge}x_{a,3,barge}}{3T_{3,barge}}\,C_{D,3,barge} = \frac{8\rho S_{3,barge}x_{a,3,barge}}{3T_{3,barge}}\,C_{D,3,platform}$$

it can be deduced as

$$b_{L,3} = b_{L,3,barge} = \frac{8\rho S_{3,barge}x_{a,3,barge}}{3T_{3,barge}}\,C_{D,3,platform}$$

for the barge,

$$\frac{b_{L,3,barge}T_{3,barge}}{S_{3,barge}x_{a,3,barge}} = \frac{8\rho}{3}\,C_{D,3,platform}$$

$$b_{L,3,barge}\frac{T_{3,barge}x_{a,3,platform}S_{3,platform}}{T_{3,platform}x_{a,3,barge}S_{3,barge}} = \frac{8\rho S_{3,platform}x_{a,3,platform}}{3T_{3,platform}}\,C_{D,3,platform}$$

then we can deduce the following equation for the platform

$$b_{L,3,platform} = b_{L,3,barge}\frac{T_{3,barge}x_{a,3,platform}S_{3,platform}}{T_{3,platform}x_{a,3,barge}S_{3,barge}} \tag{4.26}$$

At the resonant frequency, $b_{L,3,barge} = 6 \times 10^6\ kg.m^2.s^{-1}$.

The excitation amplitude $x_{a,3,barge} = x_{a,3,platform} = 1\ m$.

The natural period of the heave motion for the barge is $T_{3,barge} = \frac{2\pi}{\omega_0} = \frac{2\pi}{0.6} = 10.5\ s$

And as a reminder,$T_{3,platform} = 11.5\ s$.

Then, the estimated linear heave viscous damping is equal to: $b_{L,3,platform} = 4.73 \times 10^6\ kg.m^2.s^{-1}$

The viscous damping at this amplitude of motion is then about 2 times bigger than the wave radiation damping. The heave RAO of the damped platform is shown in Figure 4.14. This value is compared with the RAO of Geocean's OTEC platform from Deep large seawater intakes: a common solution for floating Lng in oil and gas industry and otec in marine renewable energy [13], displayed on Figure 4.15.
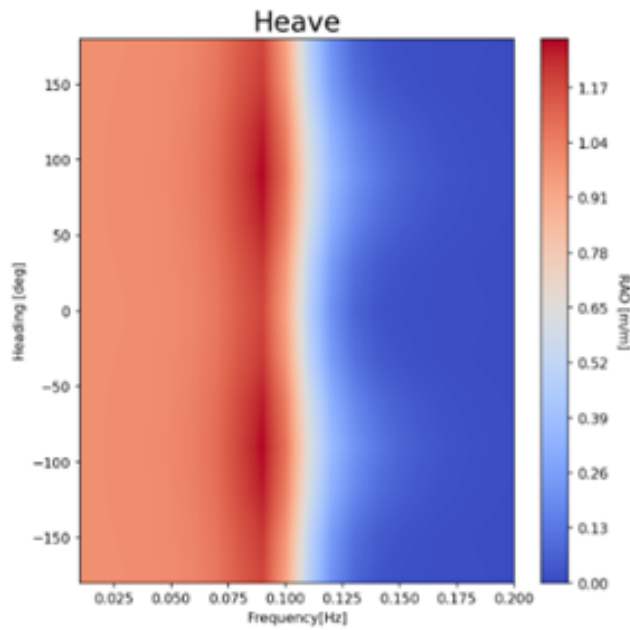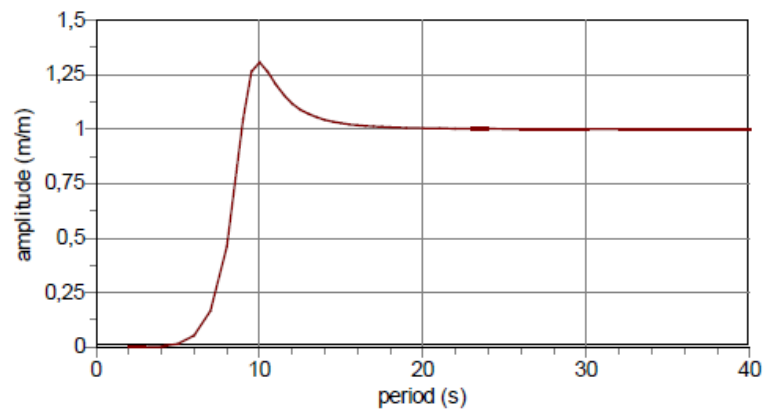
Figure 4.14: Heave RAO of the damped Platform

Figure 4.15: Heave RAO of Geocean's OTEC platform

It can first be noted that the resonant frequency of Geocean's OTEC platform from [13] is similar to our platform's. The amplitude is about 1.3 m/m as well, therefore it validates the heave damping value calculated .

Now, since the damping of the platform is determined, a complete dynamic simulation can be performed with Ansys AQWA.

4.7   Dynamic Analysis

Time domain analysis is carried out in Ansys AQWA where the software generates a time history of the simulated motions of the platform arbitrarily connected to mooring lines, under the action of wind, wave and current forces projected along the y direction of platform.

The position and velocities of the platform are calculated at each time step by integrating the accelerations due to forces in the time domain. The Time Domain response using Ansys AQWA is carried out to determine the Platform Amplitude and Mooring Line Tension. The Ansys AQWA model of OTEC Power Plant with it's mooring lines used for analysis is shown in Figure 4.16
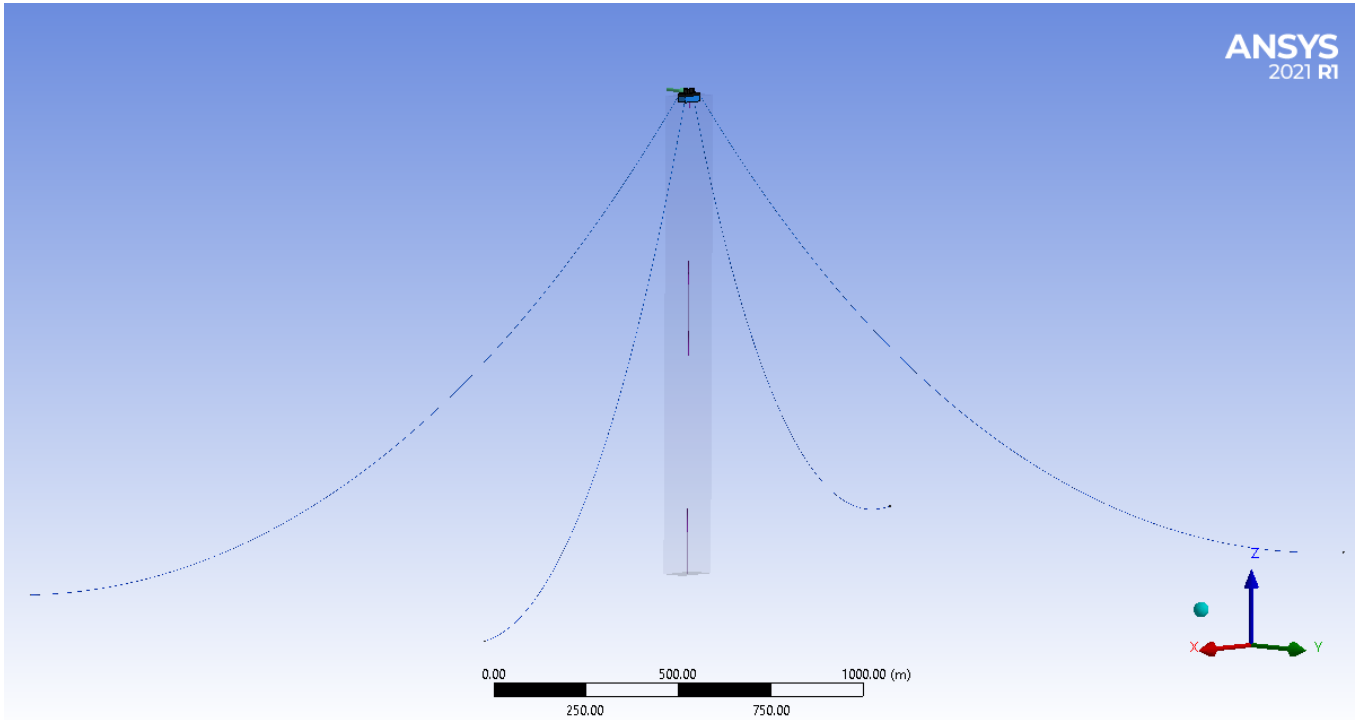

Figure 4.16: OTEC Power Plant with it's Mooring Lines in Ansys AQWA

The Mooring Line needs to sustain cyclonic conditions which are summarised in Table 4.3 and therefore, the analysis is done at cyclonic conditions under regular waves and irregular waves. However, the pipe can only sustain the operational conditions which are summarised in Table 4.2 and therefore, analysis determining the platform amplitude is carried out at operational conditions under regular and irregular waves.

Table 4.3: Cyclonic Environmental Conditions

Cyclonic Conditions	Values
Wave Amplitude	5.81 m
Current Velocity	0.4 m/s
Wind Velocity	70 m/s

4.7.1 Platform Amplitude

The platform amplitude is calculated using Ansys AQWA. The output of the AQWA model is x and z position of the center of gravity of the platform over time.

They are fitted with a sinusoidal motion as follows:

$$
\begin{aligned}
x_0 &= a_x sin\left(b_x t\right) + c_x \\
z_0 &= a_z sin\left(b_z t\right) + c_z
\end{aligned}
\tag{4.27}
$$

Thus, it permits to have a simple model to get the velocity and acceleration of the platform:

$$
\begin{aligned}
\dot{x}_0 &= a_x b_x cos\left(b_x t\right) \\
\ddot{x}_0 &= -a_x b_x^2 sin\left(b_x t\right) \\
\dot{z}_0 &= a_z b_z cos\left(b_z t\right) \\
\ddot{z}_0 &= -a_z b_z^2 sin\left(b_z t\right)
\end{aligned}
\tag{4.28}
$$

4.8   Results Under Environmental Loading

Computation of the tension in mooring lines is done to check if the tension is below the maximum limit and if the partial safety factors are respected.

4.8.1   Tension in Mooring Lines

Table 4.4, it can be seen that Line B and Line D experiences the highest tension since the environmental conditions are coming from y-axis. Since the highest tension experienced is of 3913.55 kN. In Annexure D, the cable tension experienced by all four Caternay chains are plotted.

Table 4.4: Maximum Tension Induced in each Cable with Regular Waves

Tension/Cables	Line A	Line B	Line C	Line D
Maximum Value (kN)	2682.19	3913.55	2675.44	3901.74

When the irregular waves which are more realistic waves, there is still more tension experienced in Line B and Line D as seen in Table 4.5 but lesser tension experienced than regular wave. Furthermore, the tensions in both cables have reduced compared to the case of regular wave exposure.However, the total tension experienced by the mooring system is well within the limit of the calculated/analytical total tension which ensure that the mooring lines subjected to cyclonic conditions in irregular waves are strong enough to prevent the failure of mooring cables.

Table 4.5: Maximum Tension Induced in each Cable with Irregular Waves

Tension/Cables	Line A	Line B	Line C	Line D
Maximum Value (kN)	2216.51	2869.88	2243.99	2895.31

The partial safety factor check is now carried out to ensure that the cable can withstand the Consequence Class 1 as directed by Offshore Standard DNVGL-OS-E301[11]. From the Table 4.6, the partial safety which is found to be 0.79 and 0.61 for ULS and ALS under Regular waves

which is safely under the limit of 1 as given in equation 4.22 and seen in Table 4.7 the partial safety factor for cable under regular wave for ULS and ALS conditions.

The same is true for the case of cable under irregular waves to be in the limit of a partial safety factor of 1. The values found for ULS and ALS can be seen in Table 4.7 which are 0.64 and 0.50 respectively.

Table 4.6: Partial Safety Factors for Cable Tension under Regular waves

Regular Wave					
Safety Factor	Maximum Tension (kN)	Dynamic Tension (kN)	Gamma Dynamic	Gamma Mean	Partial Safety Factor on Capacity (u)
ULS	8479	3336.7	1.5	1.1	0.79
ALS			1.1	1.0	0.61

Table 4.7: Partial Safety Factors for Cable Tension under Irregular waves

Irregular Wave					
Safety Factor	Maximum Tension (kN)	Dynamic Tension (kN)	Gamma Dynamic	Gamma Mean	Partial Safety Factor on Capacity (u)
ULS	8479	2531.11	1.5	1.1	0.64
ALS			1.1	1.0	0.50

4.8.2 Amplitude of Platform

The amplitude of motion of the platform calculated is used as an input for the cPendulum and the calculation of the motion of the pipe. The plots for the amplitude of platform motion in 6 degrees of freedom in case of regular and irregular waves are in Appenxure E Plots of sway and heave are mostly relevant and used in the code cPendulum and therefore discussed in the following sections.

Regular Waves

From the Figure 4.17 it is of interest to capture the heaving of the platform as it will induce vertical motion in the movement of CWP with platform. Due to the waves being regular, the heaving motion is more harmonic in nature.
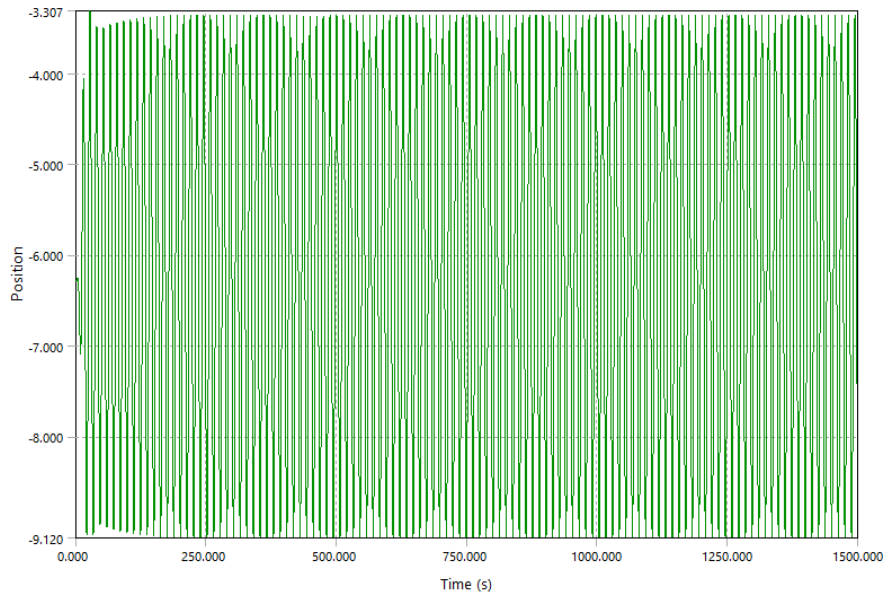
Figure 4.17: Platform Heaving with Regular waves

From the Figure 4.18 it is evident that since the applied environmental forces are coming from the y direction, the sway amplitude is the highest amongst the other degrees of freedom. Until 500 s, the platform experiences growing environmental forces and then it starts to be in a steady sway condition relative to its original axis. The offset in the motion of sway is due to the constant forces that are the wind and current.
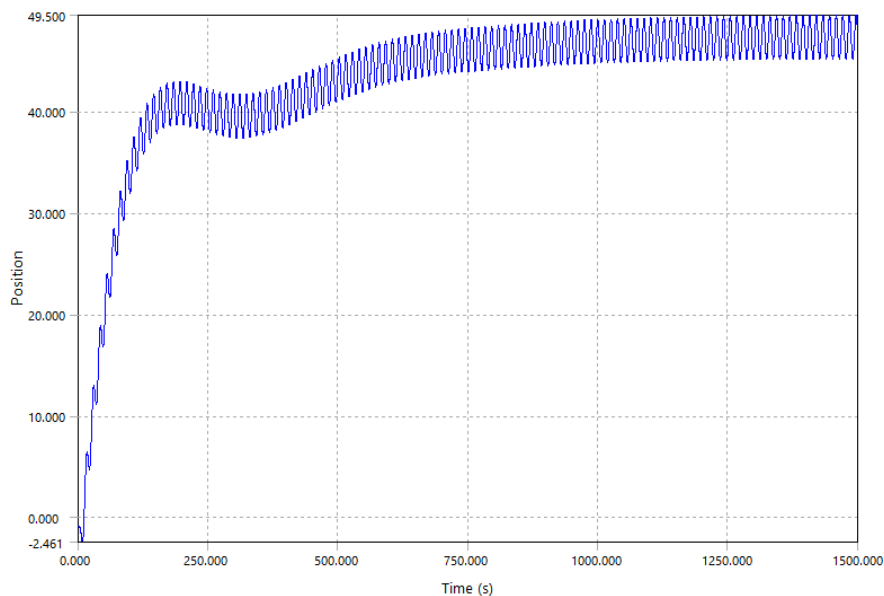

Figure 4.18: Platform Swaying with Regular waves

Irregular Waves

The platform motion in heaving condition can be seen in Figure 4.18 which induces less motion

in heave for the irregular case when compared to heave induced with regular waves since the irregular waves are not harmonic rather quite chaotic in nature.
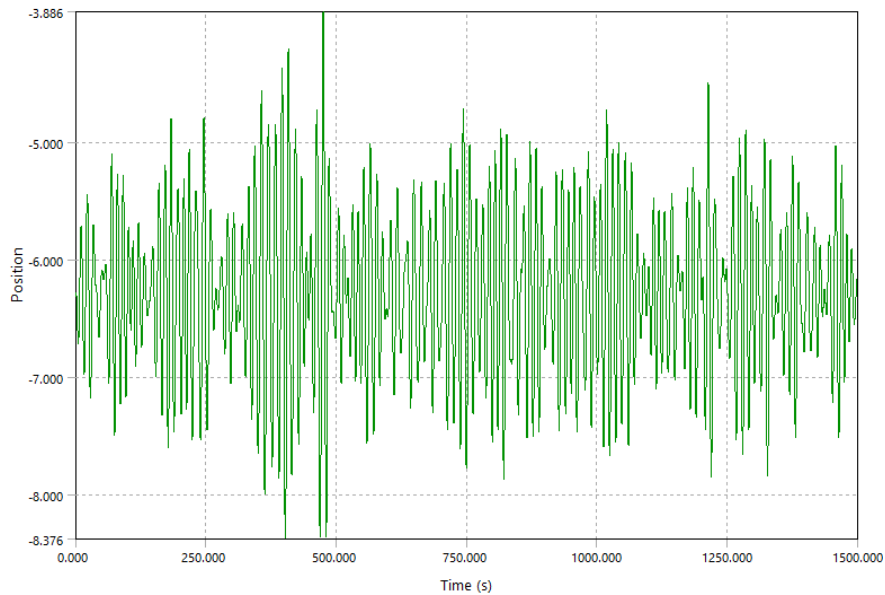

Figure 4.19: Platform Heaving with Irregular waves

The figure 4.20 shows the movements of the platform in swaying conditions due to irregular waves. It is clearly evident that the offset of swaying is higher in irregular waves compared to regular wave conditions. This uncertain behaviour may rise due to the fact that the irregular waves are quite unpredictable in nature. However, the offset in sway is higher in irregular, which is quite surprising as the offset generated from environmental loads should not differ a lot.
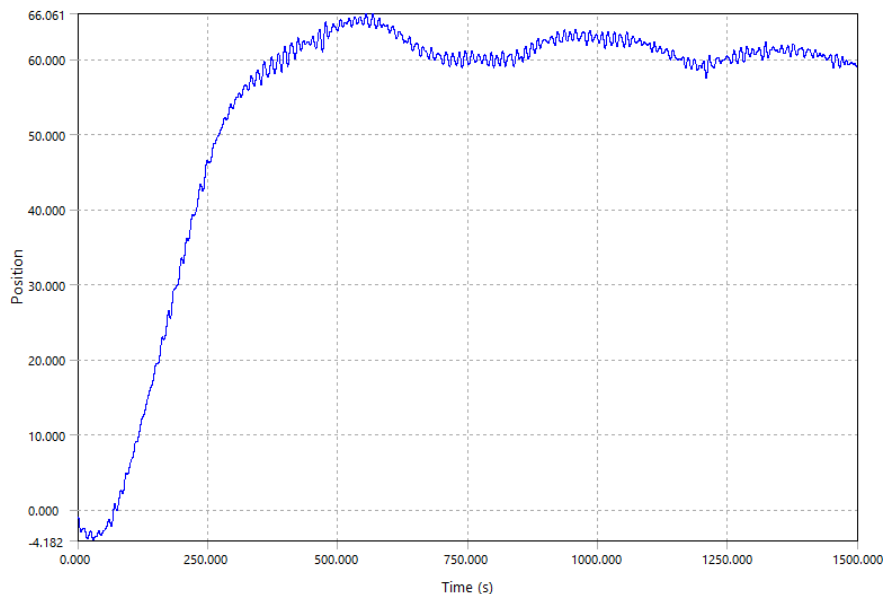

Figure 4.20: Platform Swaying with Irregular waves

The plots of surge, pitch, and yaw can be seen in Annexure E. The motion is very small in surge, pitch, and yaw because the direction of the environment is 90 degrees.

Chapter 5

Analysis of Cold Water Pipe

5.1   Analysis and Plot Description

In cPendulum code, the CWP is discretized in 100 elements of 10 meters long modules for hydrodynamic study, but the main concept of assembling modules of 1 m still remains true in terms of pipe geometry and assembly. The Pipe modules are represented with a colour spectrum that starts from red colour which represents the top module and goes until the blue colour which represents the bottom modules of the pipe. This colour spectrum helps to analyse the pipe's geometry and the impact of design loads on a specific region of the pipe.

The following plots are analysed:

- Translation Motion of Cold Water Pipe along x- axis represented as: **x[m]** in the plots

- Vertical Motion of Cold Water Pipe along z-axis represented as: **z[m]**in the plots

- Angle of deflection from the initial position represented as: **theta[rad]** plots

- Angular velocity is represented as: **thetap[rad/s]**

- Fast Fourier Transform as: **FFT[Hz]**

- Elastic Restoring Moment as: **moment[N.m]** plots

The analysis is carried out to determine the behaviour of the CWP through checking the influence of design loads separately, such as current only , waves only, platform only, and finally a coupled analysis of all loads . The three separate cases of current, waves and platform motion are studied individually first to check if their response to CWP is physical in nature. Once these cases are true individually, the coupled analysis is done with two different conditions of regular waves and irregular waves.

5.2   Current

The effect of current need to be studied for CWP design and see the motion it can induce on the CWP as currents can cause large steady excursions on the motion of CWP. In this section, the current is analysed firstly keeping it constant with depth and then changing the current along with depth as seen earlier in Figure 3.9. In the case of the current only, what is of atmost importance is whether the CWP is reaching the equilibrium after a certain period of time. This is analysed in the following sections.

5.2.1   Constant Current

The first analysis carried out is to just determine the current condition where the pipe is subjected to a constant current of 0.4 m/s throughout the water depth in the direction of positive x with v_c=0.4 m/s.

As the current is a constant overtime, then the position of CWP after the transitory state becomes a permanent state. From Figure 5.1 plots of angular velocity **thetap[rad/s]** and plot of **x[m]** shows decaying in the CWP, which further leads to zero and shows that an equilibrium is reached. This helps to understand that the current applied in cPendulum is physical and can be further used in the coupled analysis of the CWP.

(a) Plot of thetap[rad/s]

(b) Plot of x[m]
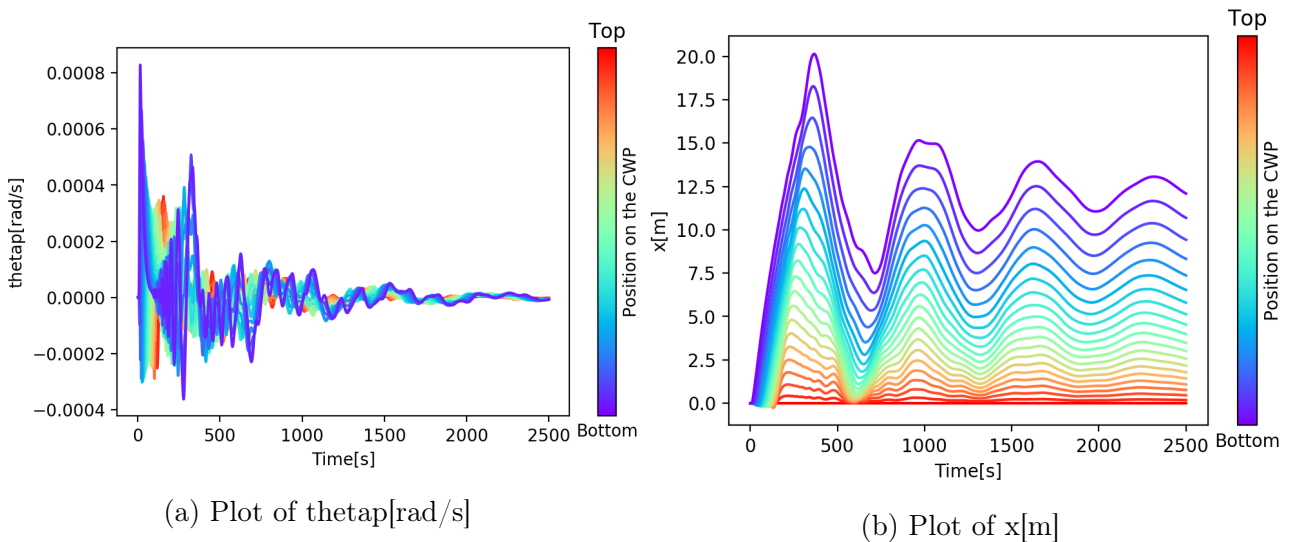
Figure 5.1: Plots for constant current

The equilibrium position is shown in the following plot:
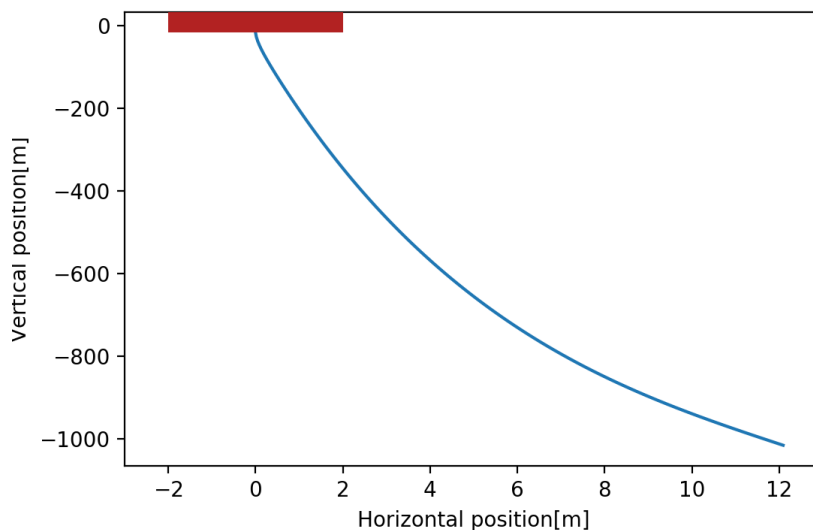
5.2.2   Current varying with the Depth

In reality, the current changes with varying depth, it is more physical to check the behaviour of CWP with current only which changes with the depth as seen earlier in Figure 3.9 and calculated from equation 3.13. From the Figure 5.2 the plots of **theta[rad]** and **x[m]** which shows that the modules are achieving equilibrium with time and clearly the decaying of the pipe is achieved.
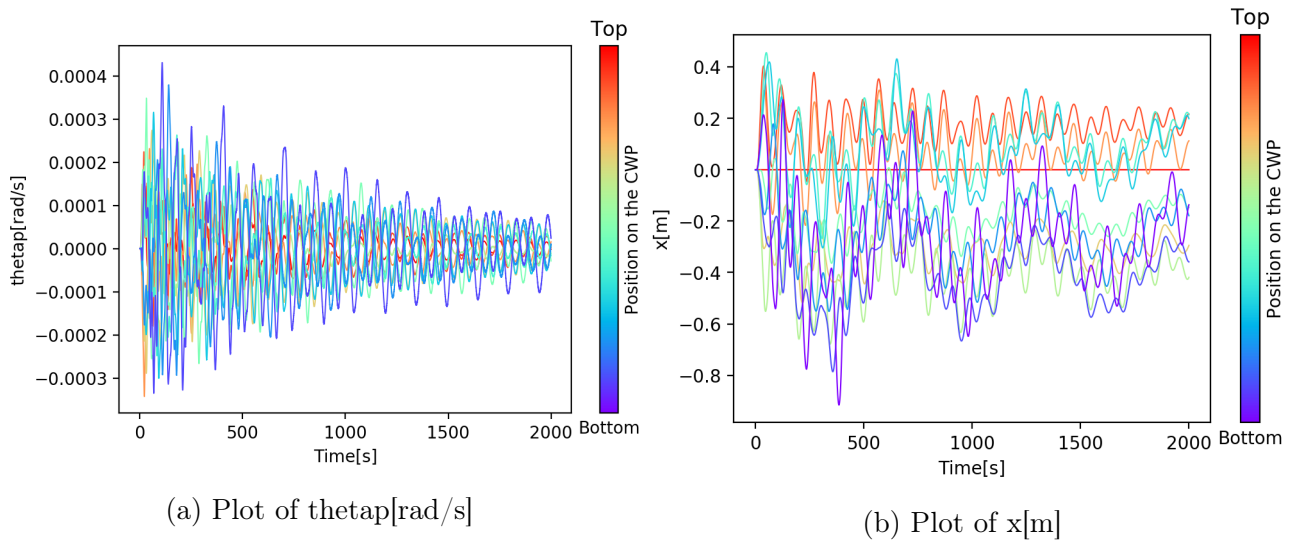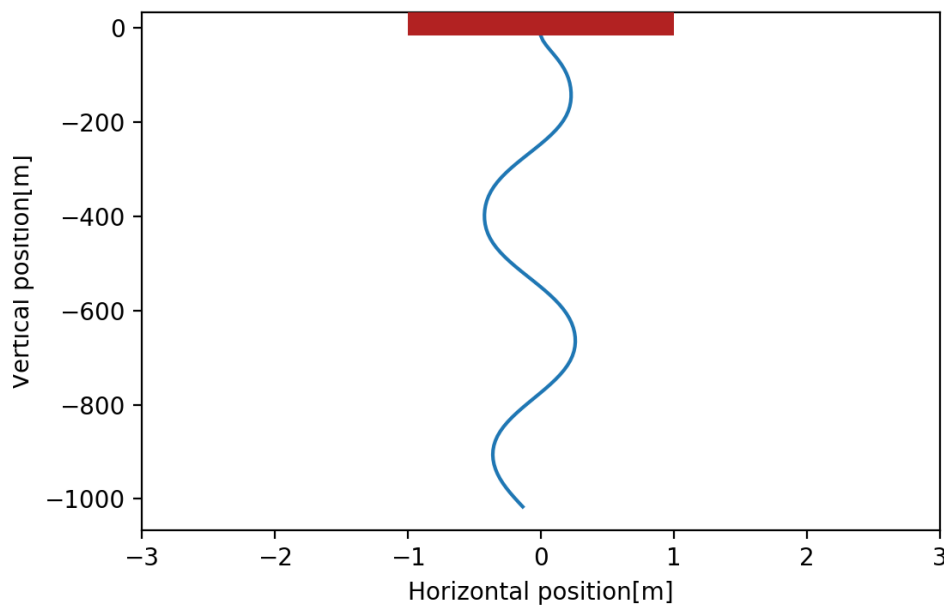

(a) Plot of thetap[rad/s]

(b) Plot of x[m]

Figure 5.2: Plots for varying current

The equilibrium position of the CWP with varying current is shown in the following plot:

5.3   Waves

The comparison between the impacts of waves types is significant to understand the behaviour of CWP. Therefore, the study of wave only is carried out on regular waves and irregular waves only, to determine the behaviour of CWP subjected to wave loads.

5.3.1   Regular Waves

Applied wave type is regular waves under operational conditions which have a wave amplitude of 2.81 m. It can be seen in Figure 5.3 from plot of **theta[rad]** that it takes 50 seconds for the motion of the pipe to reach the bottom of it. Moreover, each mass has a sinusoidal motion due to the fact that the waves are regular in nature. Furthermore, with all masses having the same frequency of motion, as seen in the **FFT[Hz]** that there is a big single peak and this frequency is the wave frequency.
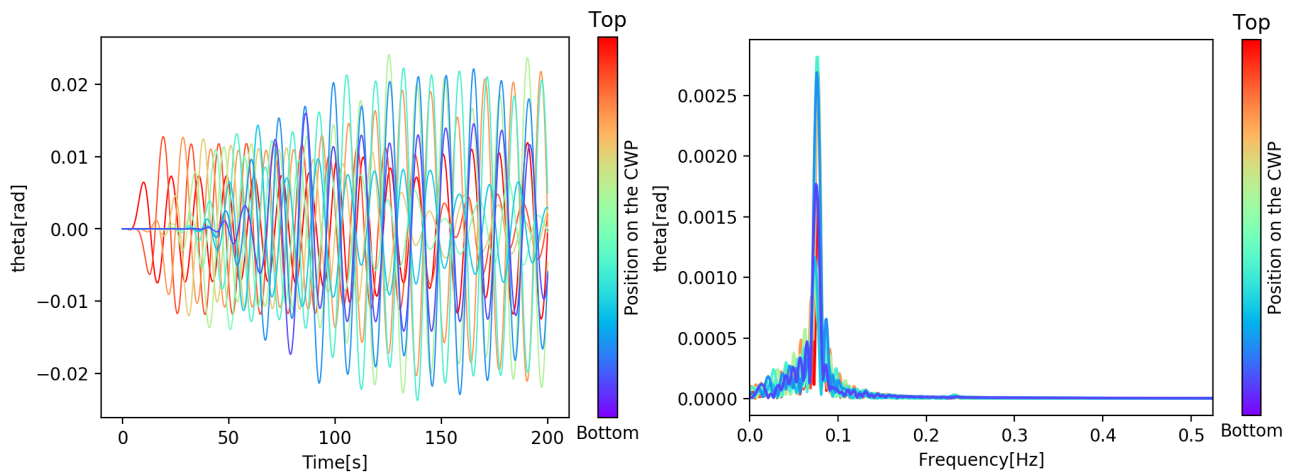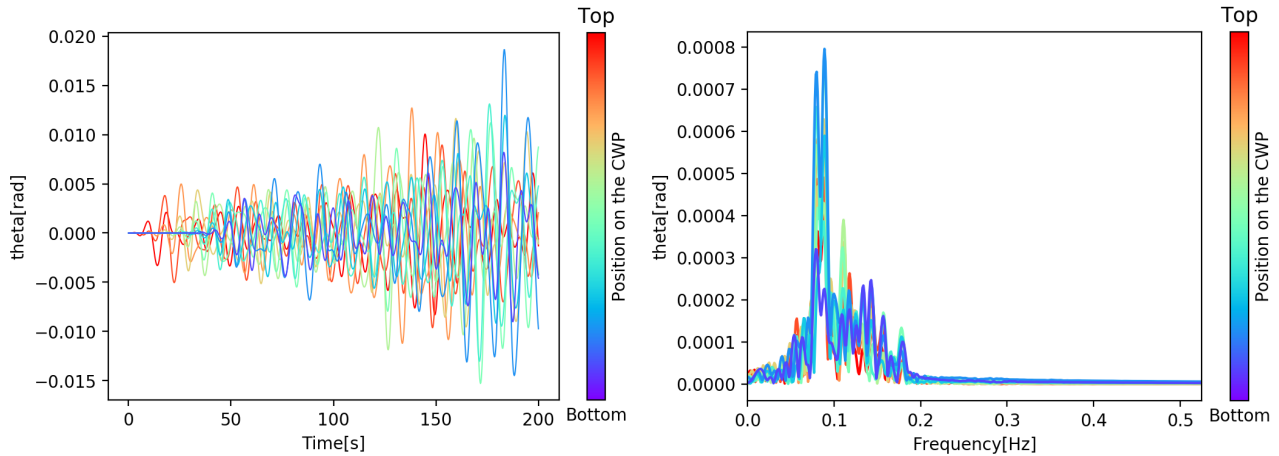

(a) Plot of Theta for Regular Waves   (b) Plot of FFT Theta for Regular Waves

Figure 5.3: Plots for Regular Waves

5.3.2   Irregular Waves

The nature of the irregular waves that are used in cPendulum is derived from the oceanic condition of Reunion Island, which makes it significant to study the response of CWP subjected to these waves.

From the Figure 5.4 in plot of **theta[rad]** it can be seen that it also takes 50 seconds for motion of the pipe to reach the bottom most module. However, compared with regular waves simulation, the motion of the masses are not perfectly sinusoidal which is completely true with irregular waves. Furthermore, with the plot of **FFT[Hz]** it confirms that there are many frequency components, and not a single peak which is expected for the case of irregular waves.

(a) Plot of Theta for Irregular Waves

(b) Plot of FFT Theta for Irregular Waves

Figure 5.4: Plots for Irregular Waves

5.4   Motion of Platform

Loads induced by the platform are expected to have the most impact on the CWP motion. The platform amplitude is mainly governed by swaying and heaving.

5.4.1   Motion of Platform Under Regular Waves

The motion of the platform influenced by regular waves induces a sinusoidal motion of the platform as seen in Figure 5.5 from plot of **x[m]**. Such motion of platform also induces a quite sinusoidal rotation of the masses.

However, there is a low frequency component induced. The simulation ran for this case is much longer time compared to Platform motion under irregular waves as the plot of **x[m]** with longer time permits to see the long periods of the motion in translation. The plot of **FFT[rad]** shows a peak at a very low frequency of 0.001 Hz as well as a peak at a wave frequency of 0.77 Hz.
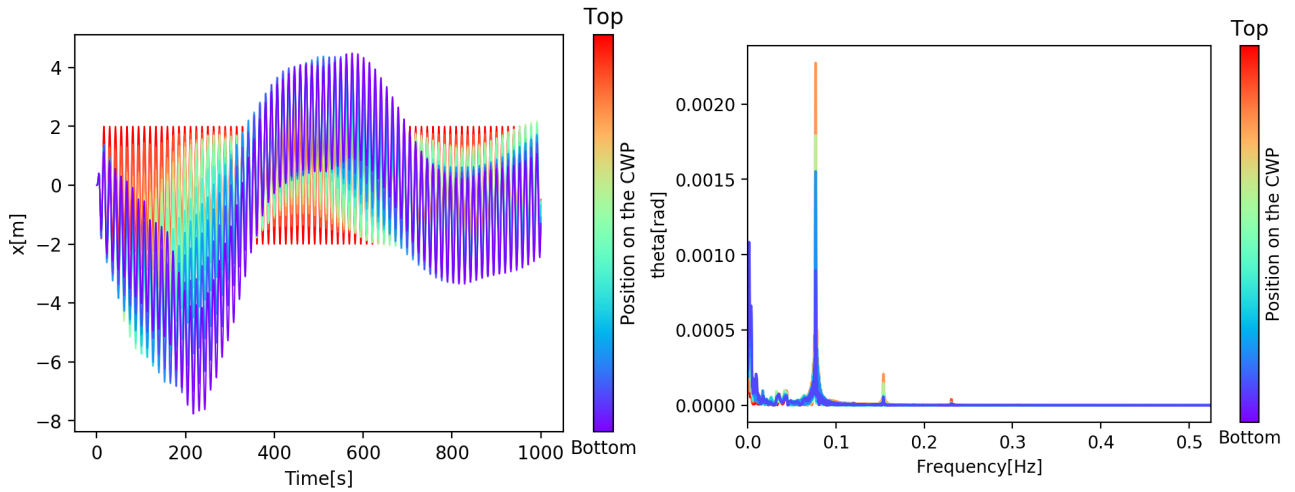
Figure 5.5: Plots for Platform Motion under Regular waves

5.4.2   Motion of Platform Under Irregular Waves

The motions induced in CWP due to platform amplitude are a sum of sinusoids since the platform is under irregular waves and this can be seen in plot of **theta[rad]** in Figure 5.6. The Impact of heaving motion and swaying motion of the platform can be seen on the top modules in the plot of **theta[rad]** where the heave motion makes the platform move up and down with the platform under swaying condition induces motion directly at the top modules. The motion of the platform induced the translation of motion in CWP as shown in the plot of **x[m]** which is quite physical, and these platform conditions can be used for couple assessment.
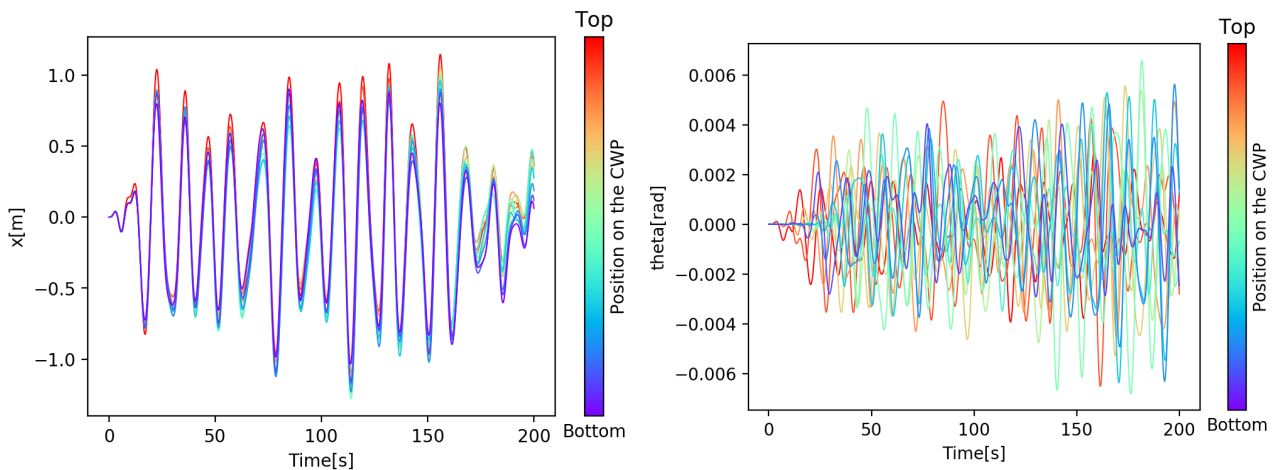

Figure 5.6: Plots for Platform Motion under Irregular waves

5.5   Coupled Analysis of CWP

From the previous case studies of motion induced by CWP through various individual load cases, it can be said that the impact between these load cases needs to be applied together to know the real behaviour of the CWP when subjected to various design loads.

In this section, the behaviour of CWP in regular waves is compared to irregular waves to determine the motion induced by changing wave type.

To compare the Regular Wave and Irregular Wave, the regular waves have a similar wave amplitude with the operational significant wave height, and the wave elevation under regular and irregular waves is given in Figure 5.7. Furthermore, to model the impact of waves on CWP, the platform amplitude is taken from the section and a constant current of 0.4 m/s.
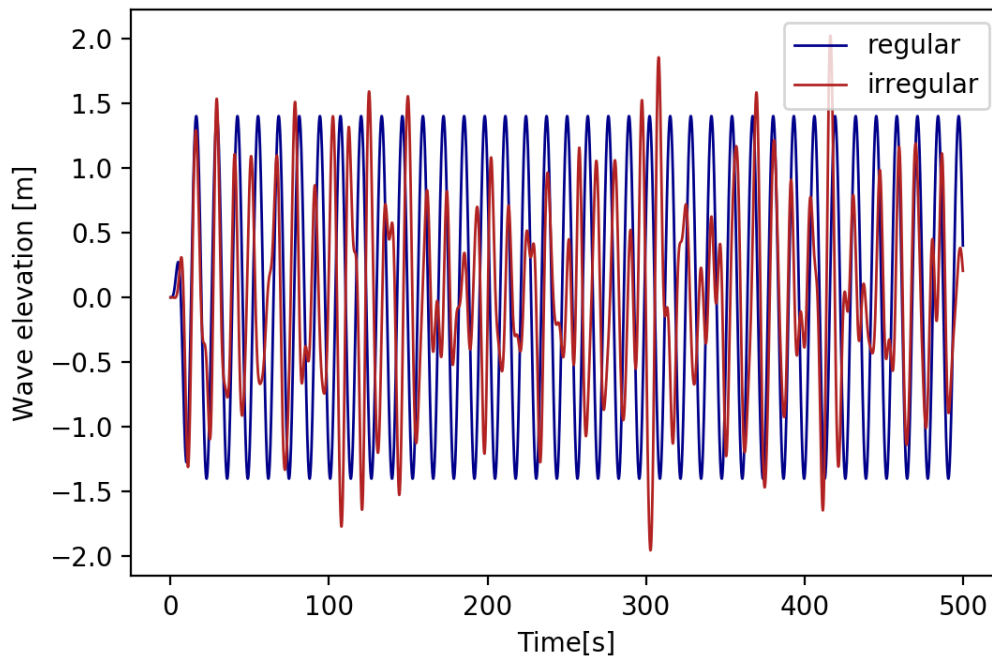

Figure 5.7: Wave Elevation for Regular and Irregular Wave

5.5.1   Regular Waves

Coupled analysis is carried out on all considered design loads with the case of regular waves. From the plot of **x[m]** in Figure 5.8 the pipe seems to have a proper sinusoidal behaviour as expected due to regular waves and the platform near the water surface impact's initial behaviour of the pipe which gets amplified at each oscillation with a constant current effecting the lower modules.

From plot of **theta[rad]**, the lower modules experiences the highest translation motion as the pipe is free at the lower end which receives the highest load propagation from waves, platform and current combined. Furthermore, from plot of **FFT[Hz]** of regular wave, there is a peak at 0.77 Hz which is a result of wave and platform and a peak at around 0 Hz which comes from

the excitation constant over time of current and can be said that the CWP receives a strong influence of current. However, there is no significant vertical motion induced by any of the loads which can be seen in plot of **z[m]**.
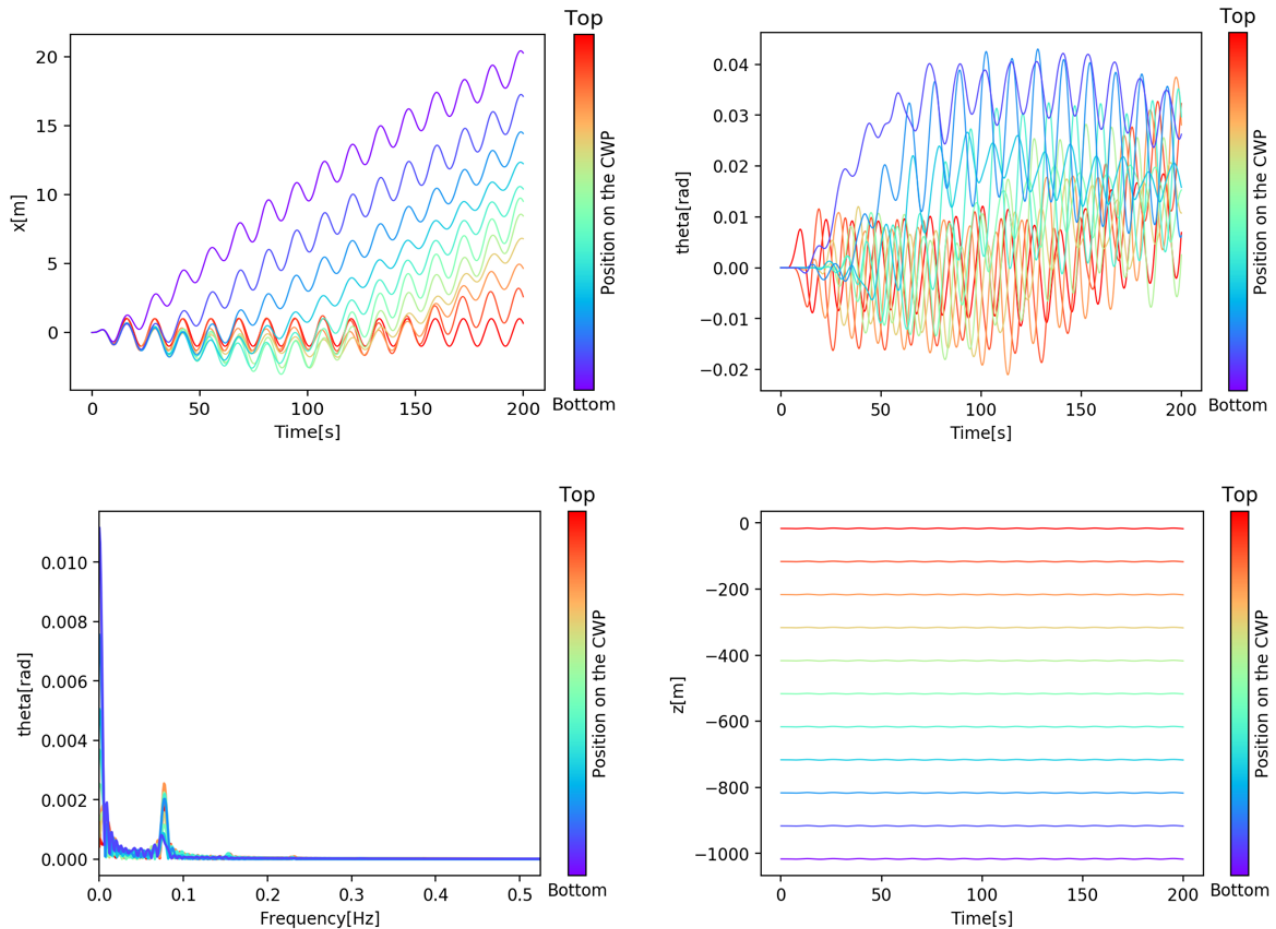

Figure 5.8: Plots of Coupled Analysis of CWP

5.5.2   Irregular Waves

The coupled analysis under irregular waves induces the motion of CWP which is not properly sinusoidal in motion as the wave induced by the swell and the platform is a sum of many waves of different frequencies. Due to this fact, the components of the swell and platform motion are sometimes in opposition to the phase of the wave and can be seen the impact on the top modules from plot of **theta[rad]** in Figure 5.9 where the angles of deflection from the initial position in top modules is lower than the regular waves.

Furthermore, there is no peak around 0.77 Hz in plot of **FFT[Hz]** which may be true as the wave going downwards in the pipe is a sum of waves of higher and lower frequencies and thus a sum of waves of different frequencies and velocities compared to the wave going downwards in regular case and therefore the regular waves have a peak and irregular does not have one. However, there is also no significant vertical motion induced by any of the loads which can be seen in plot of **z[m]**.
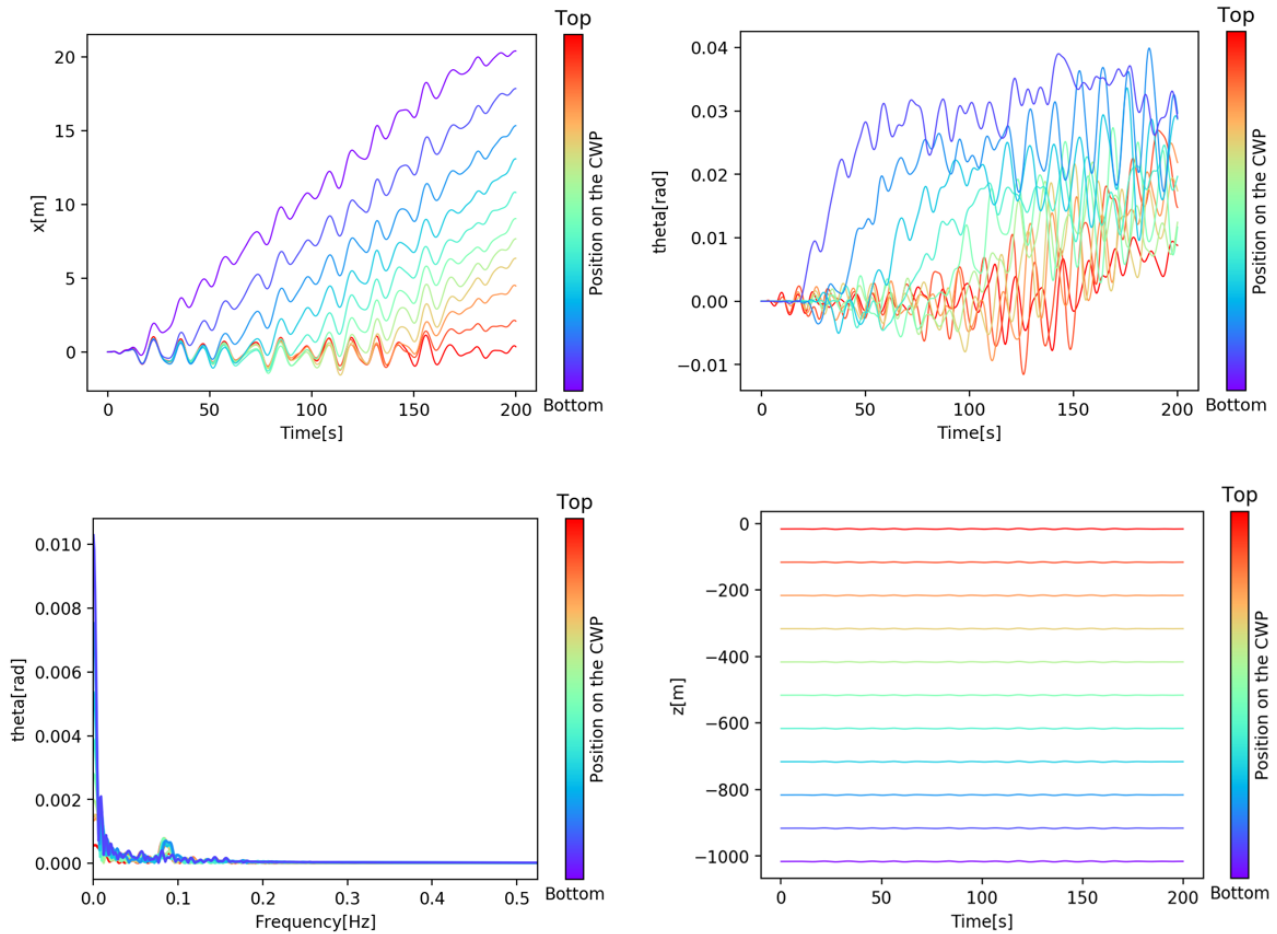
Figure 5.9: Plots of Coupled Analysis of CWP under irregular waves

5.6 Plots of Moments

The moments are calculated which are the final output from the hydrodynamics study carried out in this thesis. The moment is the basis for the structural studies because the moment induces tension in the stiffeners which connects the modules, which in turn effects the size of the stiffeners and finally effects the weight and strength of the local connection between each module. The moment calculated for coupled analysis of OTEC plant with CWP under regular waves is shown in Figure 5.10 and the moment calculated for coupled analysis of OTEC Plant and CWP under irregular waves is shown in Figure 5.11.
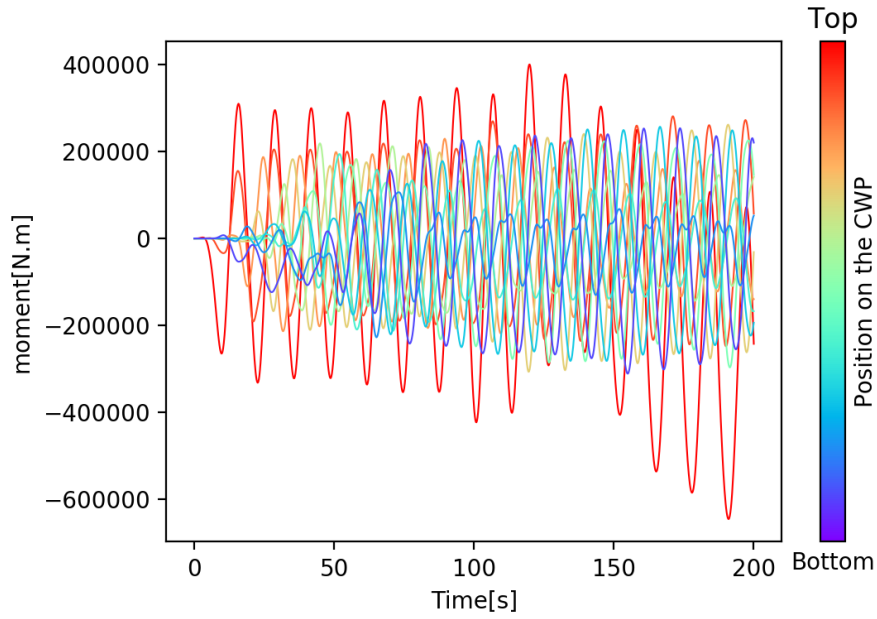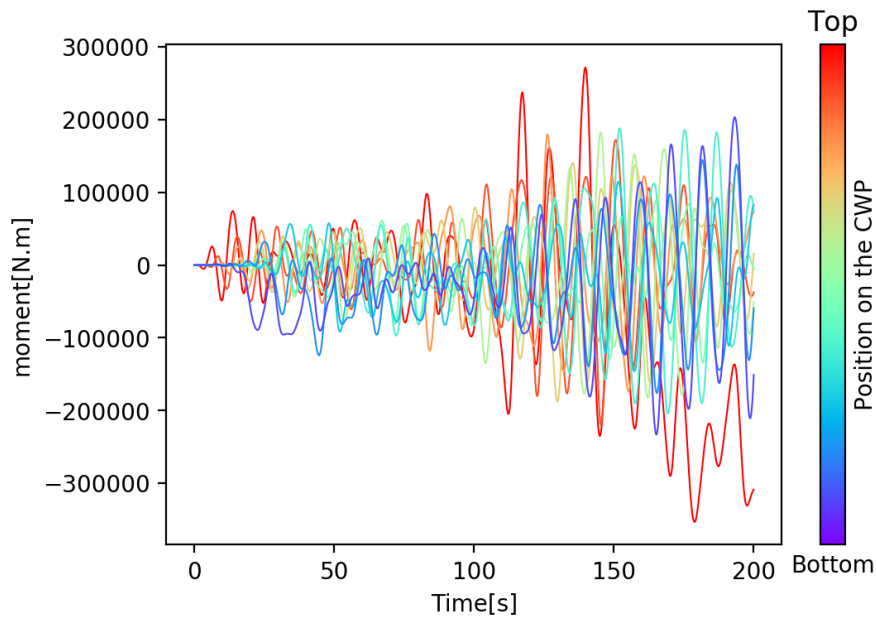
Figure 5.10: Moment from Regular waves

Figure 5.11: Moment from Irregular waves

Chapter 6

Conclusions

The dynamic analysis of CWP which coupled to OTEC plant which is of a paramount importance for CWP design.This study will have allowed the DEEPRUN project to evolve over time towards a reliable global behaviour of CWP under hydrodynamic loads, which builds the basis of the detail structural study of local connections between each module of the pipe. In this thesis, the initial hydrodynamics parameters that impact the motion of CWP have been studied, which consists of the hydrodynamic coefficient, motion of the platform and mooring system, hydrodynamics forces and finally calculating the moment induced.

The code cPendulum has been built and successfully used to model the behaviour of the CWP which helped to understand in detail about the motion induced due to the Hydrodynamic forces. Furthermore, the analysis is carried out for regular waves and irregular waves along with current velocity and motion induced by platform amplitude.Furthermore, a proper mooring system is being designed such that it resists the tropical storms that the platform may be subjected to.

A hydrodynamic time response simulation has been carried out to properly capture the loads induced by the environmental conditions on mooring cables, platform motion, and CWP. This coupled analysis helped to model the behaviour of CWP in real seastate to make a reasonably accurate prediction of likelihood of the RUNETM's CWP.

The foundations of the concept are now sound and the main lines have been drawn. The continuation of this work which will be carried out further design loops which will eventually lead to the production of the first deep cold water pumping pipe based on the Low-tech concept.

Chapter 7

Recommendations for Future Work

The further works that can be carried on are as follows :

- Study of the ideal value of stiffness , damping, and the attached clamped weight at bottom of the pipe.

- Improvement in Platform's hull and mooring system

- Determination of Vortex Induced Vibrations through a CFD study

- Tank test to determine and verify the hydrodynamic coefficients and damping

- Hydrodynamic Modelling using commercial software like Orcaflex or Deeplines for validation of code cPendulum

- Study of fatigue strength of the connecting stiffeners between modules

Bibliography

[1] Sandrine Selosse, Sabine Garabedian, Olivia Ricci, and Nadia Maïzi. The renewable energy revolution of reunion island. *Renewable and Sustainable Energy Reviews*, 89:99–105, 2018.

[2] Tu Delft. Thermal Gradient (OTEC). `https://www.tudelft.nl/oceanenergy/research/thermal-gradient-otec`.

[3] Arne Nestegård, Marit Ronæss, Øistein Hagen, Knut O Ronold, and Elzbieta Bitner-Gregersen. New dnv recommended practice dnv-rp-c205 on environmental conditions and environmental loads. In *The Sixteenth International Offshore and Polar Engineering Conference*. OnePetro, 2006.

[4] KJ Heywood, ED Barton, and GL Allen. South equatorial current of the indian-ocean-a 50-day oscillation. *Oceanologica acta*, 17(3):255–261, 1994.

[5] Sighard F Hoerner. Fluid-dynamic drag. *Hoerner fluid dynamics*, 1965.

[6] Xi-feng Gao, Wan-hai Xu, Yu-chuan Bai, Hai-tao Zhu, et al. A novel wake oscillator model for vortex-induced vibrations prediction of a cylinder considering the influence of reynolds number. *China Ocean Engineering*, 32(2):132–143, 2018.

[7] First Edition, JMJ Journée, and WW Massie. Offshore hydromechanics, 2001.

[8] United States Naval Academy. The input: Waves. `https://www.usna.edu/NAOE/_files/documents/Courses/EN455/AY20_Notes/EN455CourseNotesAY20_Chapter3.pdf`.

[9] Subrata Kumar Chakrabarti. *Hydrodynamics of offshore structures*. WIT press, 1987.

[10] Vicinary. Mooring chain data sheet. `https://www.vicinaycadenas.net/mooring-chain/offshore-mooring-chain.asp`.

[11] GL DNV. Offshore standard dnvgl-os-e301. *Position mooring*, 2015.

[12] Muhammad Zahir Ramli, Pandeli Temarel, and Mingyi Tan. Hydrodynamic coefficients for a 3-d uniform flexible barge using weakly compressible smoothed particle hydrodynamics. *Journal of Marine Science and Application*, 17(3):330–340, 2018.

[13] Franck Rogez. Deep large seawater intakes: a common solution for floating lng in oil & gas industry and otec in marine renewable energy. In *4th International Conference in Ocean Energy, Dublin, 17th October*, 2012.

Appendix A

Hydrodynamic Coefficients

The corresponding geometries referred to determine the Drag Coefficient of DNV-GL Recommended practices are shown in Figure A.1 and Figure A.2

Geometry	Drag Coefficient		
	L_o/D_o	C_D	
	0.5	1.8	Fore and aft corners not rounded
		1.7	
		1.7	
	1	1.5	
		1.5	
		1.5	
	2	1.1	Lateral Corners not rounded
		1.1	
		1.1	

Figure A.1: Diamond with rounded corners

Due to symmetry in the Pipe's geometry, the Lo/Do is found to be 1 which corresponds to Drag Coefficient of 1.5 in FigureA.1

Geometry	Drag Coefficient	
	Type($R_e=10^4$-10^7)	C_D
	Wire Strands	1.5-1.8
	Wire , spiral no sheating	1.4-1.6

Figure A.2: Wire and Strands

The Cold Water Pipe is surrounded by connecting stiffeners which is can be considered as strands, and therefore, the Figure A.2 shows the drag coefficient to be around 1.5-1.8.

The Figure A.3 shows the corresponding geometry used as a reference in DNG-GL to determine the added mass coefficient.

Figure A.3: Added Mass Coefficient of Circular Cylinder

Appendix B

Mooring Chain

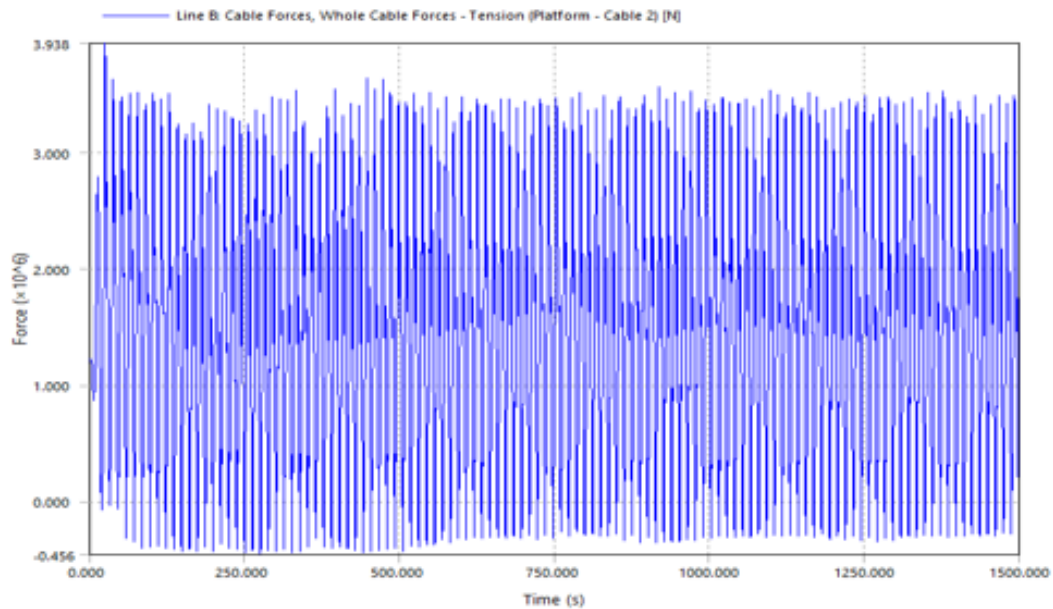The Mooring chain data sheet is taken from Vicinay[10]

Appendix C

RAO of Platform

Platform's RAO
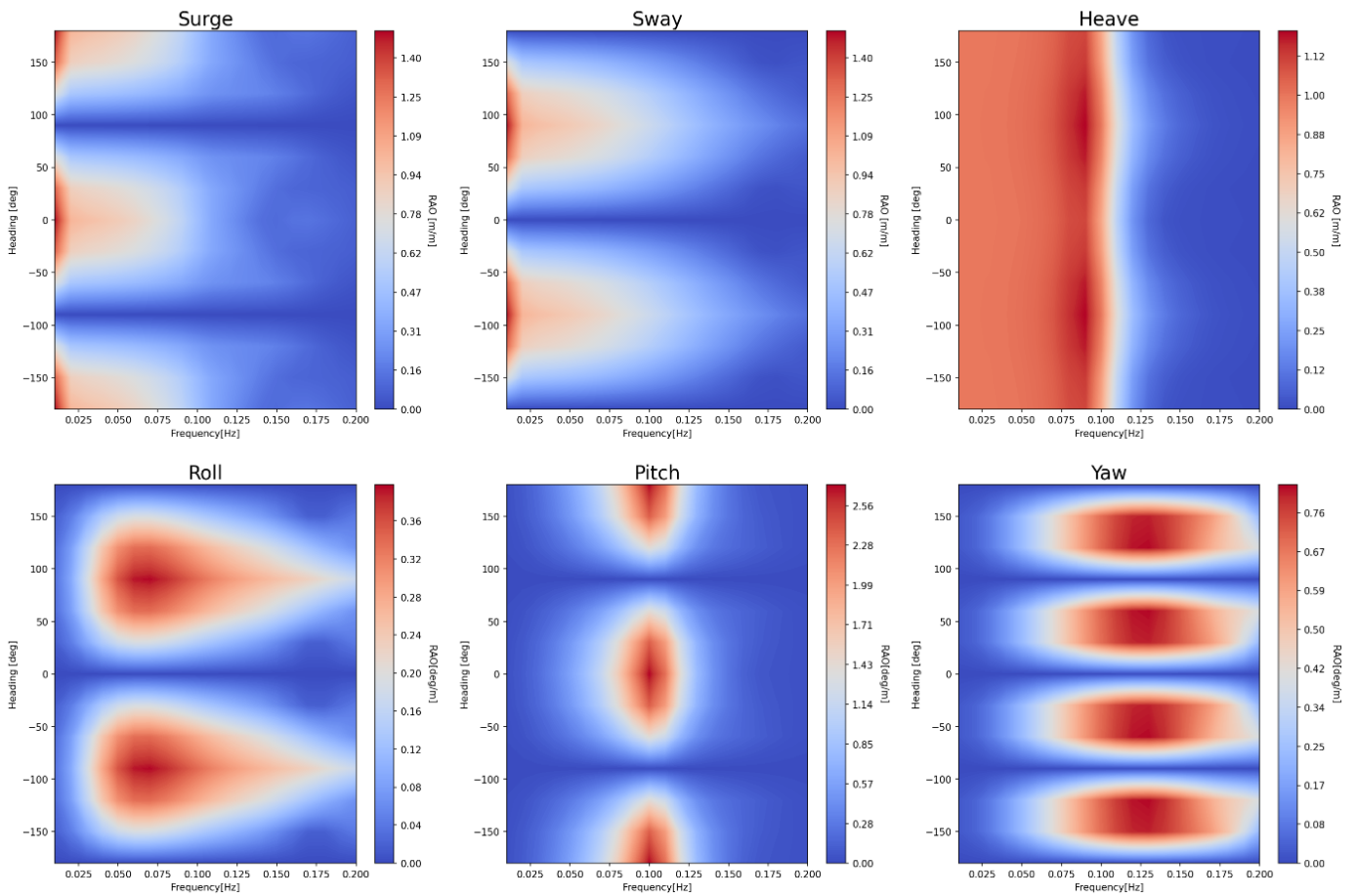
Appendix D

Tension in Mooring Cables

Line C: Cable Forces, Whole Cable Forces - Tension (Platform - Cable 3) [N]

Line D: Cable Forces, Whole Cable Forces - Tension (Platform - Cable 4) [N]
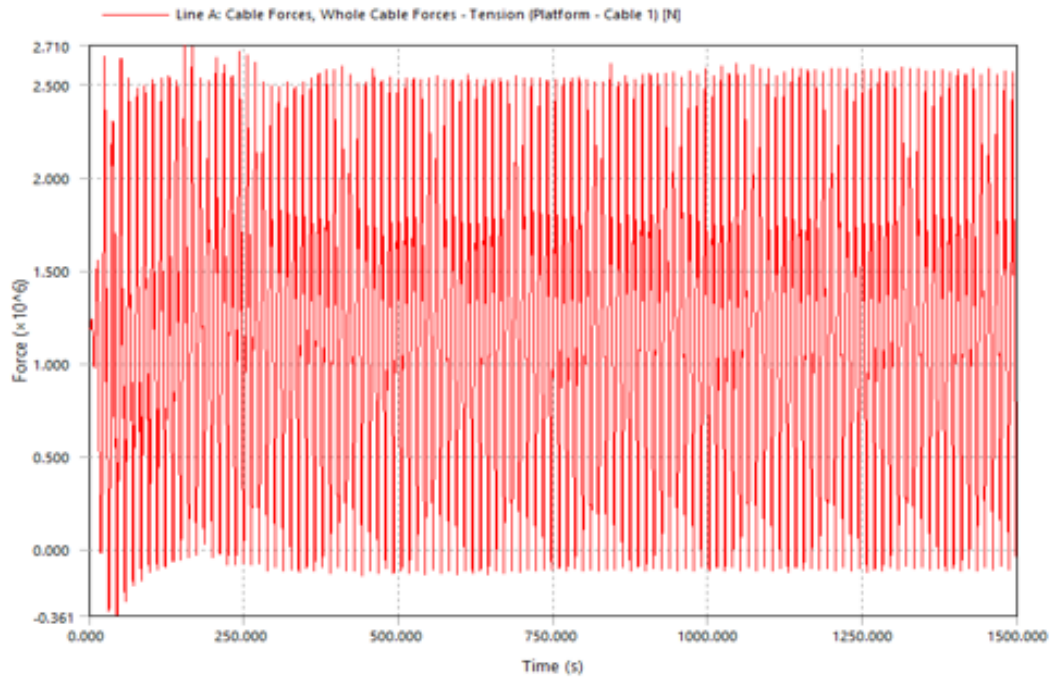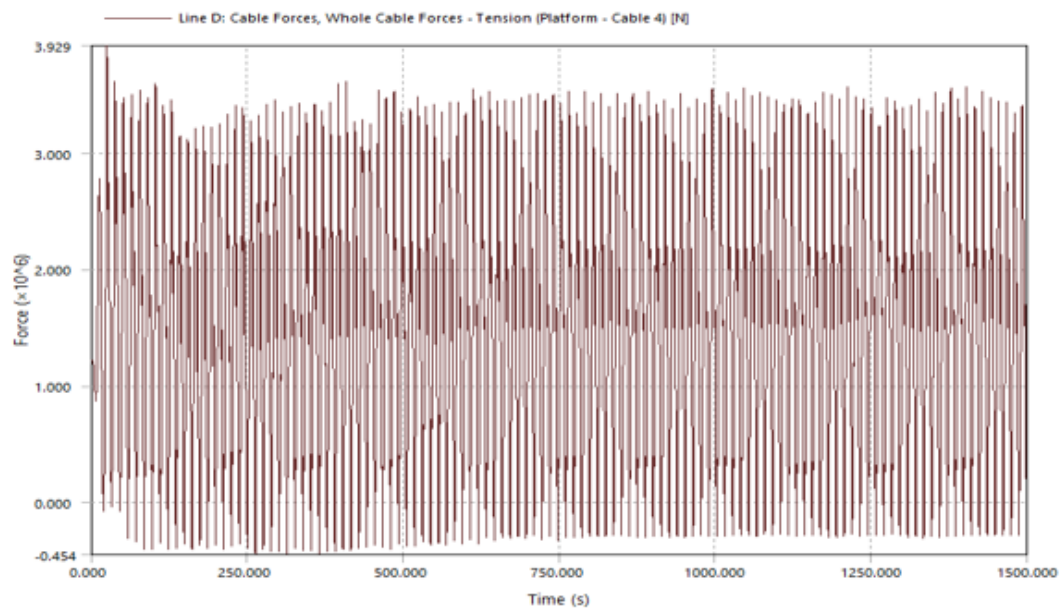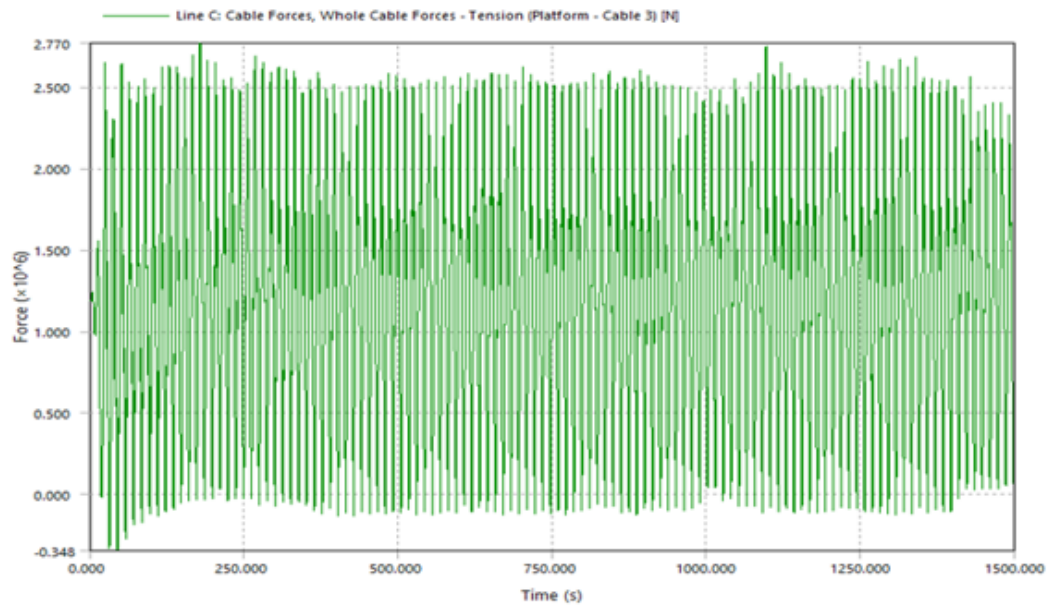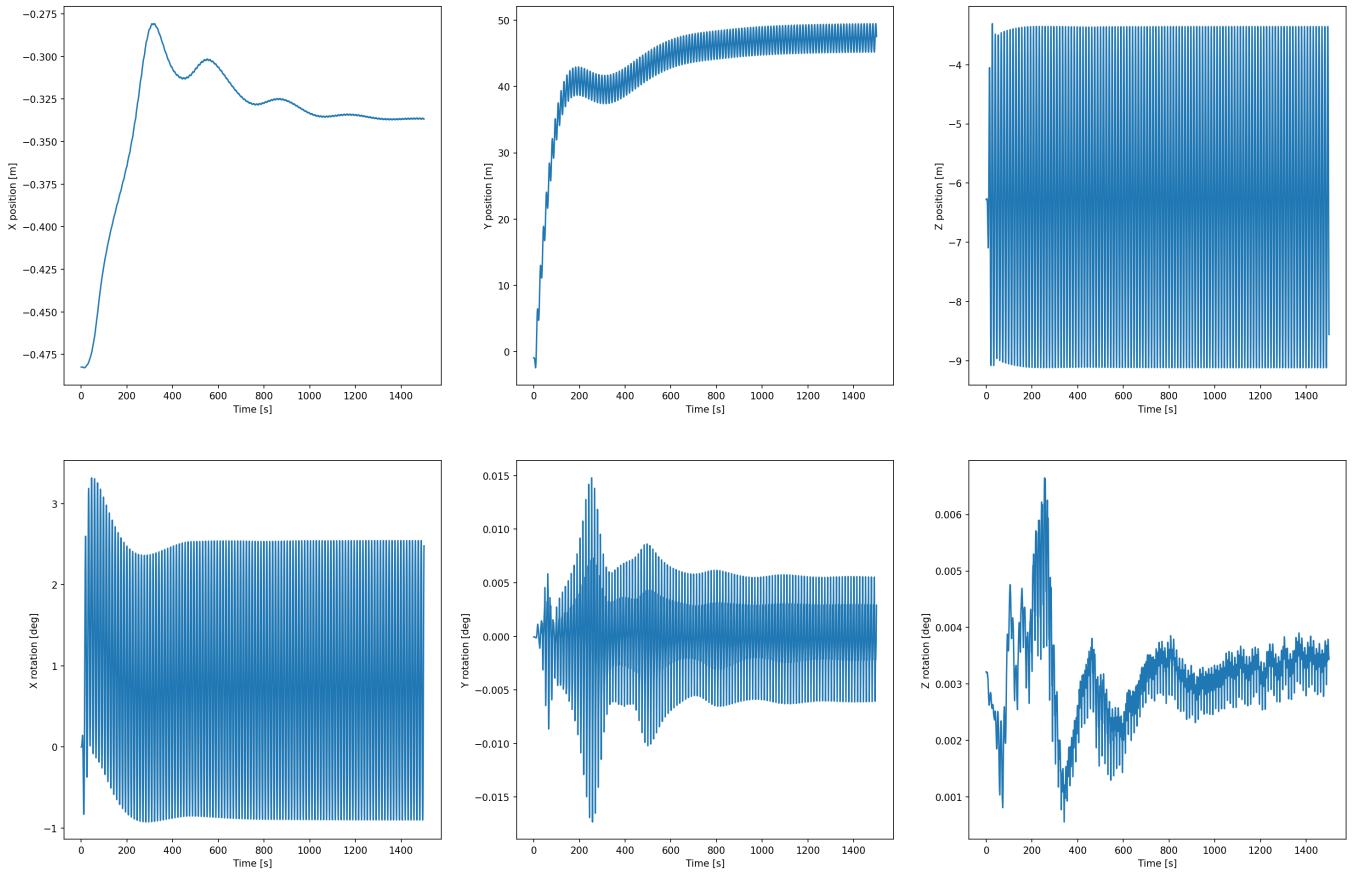
Appendix E

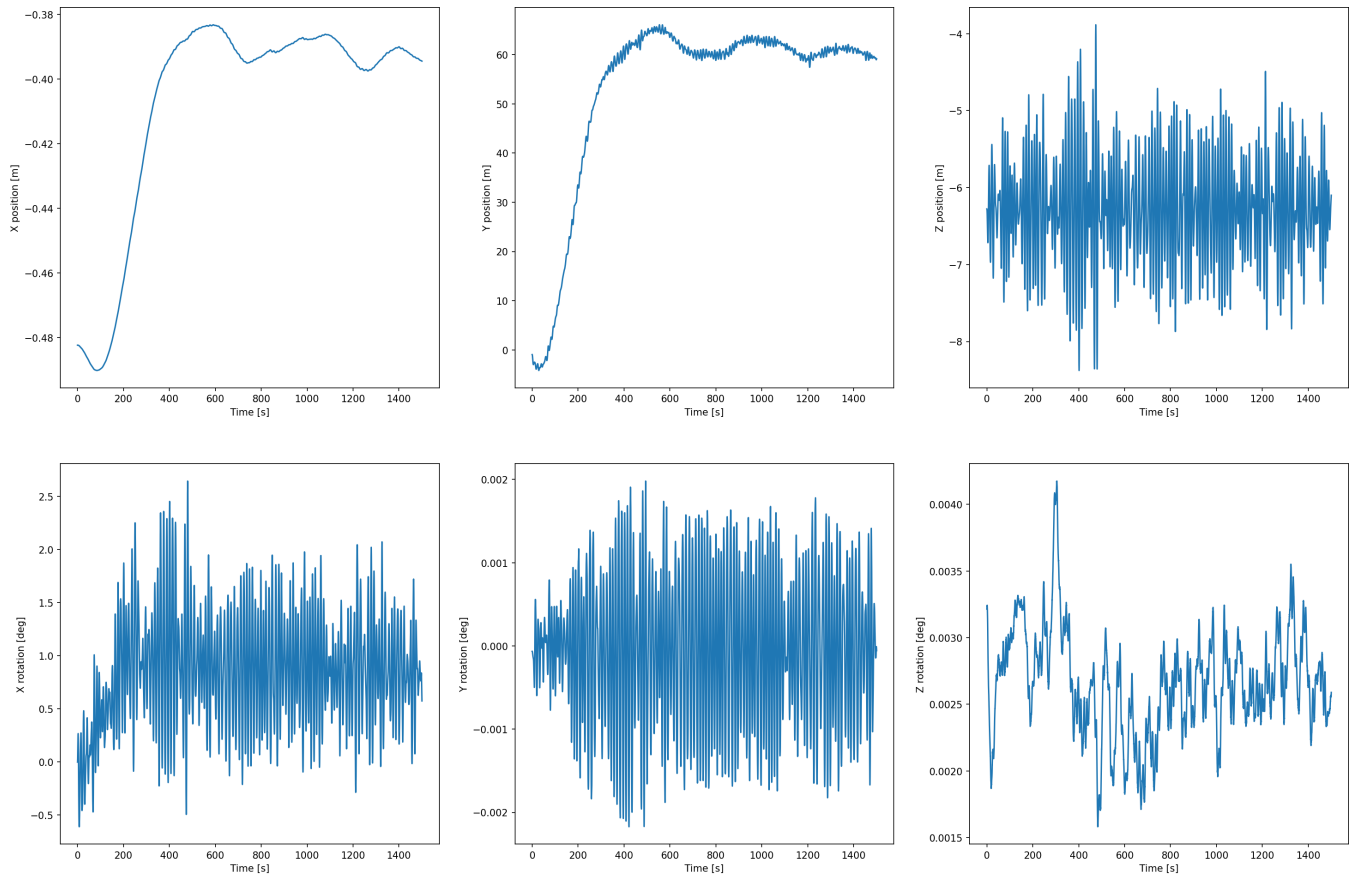# Platform Amplitude

Figure E.1: Platform Amplitude with Regular Waves

Figure E.2: Platform Amplitude with Irregular Waves